LAPPEENRANTA UNIVERSITY OF TECHNOLOGY
Faculty of Chemical Technology
Master's Degree Programme in Chemical and Process Engineering

PRODUCTION OF BIOFUELS BY FISCHER TROPSCH SYNTHESIS

Examiners: Professor D. Sc. (Tech.) Ilkka Turunen
Professor D. Sc. (Tech.) Esa Vakkilainen

Lappeenranta 2011
Peter Mponzi
Käppäratie 9 as 8
28120 Pori
Phone: +358 504 675 630

ABSTRACT

LAPPEENRANTA UNIVERSITY OF TECHNOLOGY

Faculty of Chemical Technology
Master's Degree Programme in Chemical and Process Engineering

Author: Peter Mponzi

Production of Biofuels by Fischer Tropsch Synthesis

Master's thesis

Year: 2011

Pages 91, Figures 22, Tables 16

Examiners: Professor D. Sc. (Tech.) Ilkka Turunen

Professor D. Sc.(Tech.) Esa Vakkilainen

Keywords: Fischer Tropsch Synthesis, Biomass Gasification, Tars, Gas Cleaning,

Production of biofuel via biomass gasification followed by Fischer Tropsch synthesis is of considerable interest because of the high quality of fuels produced which do not contain sulphur and are free of carbon dioxide. The purpose of this Master's thesis is to study feasibility production of biofuels integrated with Fischer Tropsch process using Aspen Plus simulation. The simulation results were used to size process equipment and carry out an economic evaluation. The results show that lowering the reactor temperature from 1000 ^{o}C - 850 ^{o}C and raising the water gas shift temperature from 500 ^{o}C - 600 ^{o}C can improve overall gas efficiency, which in turn leads to better production of ultra clean syngas for the Fischer Tropsch synthetic reactor. Similarly, the Fischer Tropsch offgas is converted into a gas turbine for power production, and finally biodiesel is produced as fuels for transportation.

ACKNOWLEDGMENTS

The research for this Master's Thesis was conducted at two Departments of Lappeenranta University of Technology, the Department of Chemical and Process Technology, supervised by Professor Ilkka Turunen and the Department of Energy and Environmental Technology, supervised by Professor Esa Vakkilainen. The thesis work was carried out from January 2010 to June 2011.

This thesis would not have been possible without the support of many people. First and foremost, I would like to thank my supervisor, Professor Esa Vakkilainen, for his intellectual supervision, continuous support, endless patience, motivation and encouragement through my graduate studies. I am indebted for the time he spent on helping with every aspect of research, for his invaluable suggestions and supportive guidance. I am grateful to have Professor Esa Vakkilainen as my supervisor. Working with Professor Vakkilainen exposed me to many invaluable experiences that I will deeply cherish for the rest of my life.

I would like to thank Professor Klaus Niemelä and, Ilkka Hannula from VTT Technical Research Centre of Finland, Department of Biomass and Biorefinery, and Robin Zwart from Energy Research Center of the Netherlands (ECN), Department of Biomass, for their contribution during the literature study survey.

I would like to thank my supervisor, Professor Ilkka Turunen for the comments and suggestions. I acknowledge the financial support I have received from the Research Foundation of Lappeenranta University of Technology (Lappeenrannan Teknillisen Yliopiston Tukisäätiö). Finally, I would like to express my gratitude to my family and friends who have been there for me during this long project.

TABLE OF CONTENTS

LIST OF TABLES 5
LIST OF FIGURES 5
1. INTRODUCTION 6
1.1. BACKGROUND 7
1.2. GOALS 8
2. BIOMASS GASIFICATION 9
2.1. Small Scale Gasifiers 11
2.2. Large Scale Gasifiers 12
2.3. Advantages of Circulating Fluidized Bed Gasifiers 15
2.4. Heat Transfer in a Circulating Fluidized Bed Gasifiers 16
2.5. Entrained Flow Gasification 27
2.6. Biomass pre-treatment 28
2.7. Drying of Biomass 29
3. FISCHER –TROPSCH SYNTHESIS 30
3.1.1. Synthesis 32
3.1.2. Catalysts 34
3.1.3. Water Gas Shift Reaction 34
3.1.4. Product Distribution 36
4. PROCESS DESCRIPTIONS 38
4.1. Tar Treatment Technologies 40
4.1.1. Thermal Cracking of Tars 41
4.1.2. Physical Tars Removal 43
4.1.3. Catalytic Tars Removal 43
4.2. Cleaning of Syngas 44
4.2.1. Particulate Cleaning 45
4.2.2. Acidic Gas Removal 45
5. MODELLING OF BIOMASS GASIFICATION 47
5.1. Model Mechanism 49
5.1.1. Derivation of Fluid-dynamic Model Equation 51
5.2. Aspen Plus Modeling 58
5.2.1. Energy and Material Balance 58
5.3. Process Design Specifications 63
5.4. Components Model and Equipment Specifications 64
5.4.1. Aspen Plus Simulation Results 65
5.4.1.1. Simulating the Wood Feed Stream 65
5.4.1.2. Simulating the Wood Gasifier 65
5.4.1.3. Sensitivity Analysis 69
5.4.1.3.1. Effect of Temperature on Gasifier 69

5.4.1.3.2. Effect of Temperature on Heating Value 70
5.4.1.3.3. Effect of Temperature on Water Gas Shift Reactor 71
5.4.1.3.4. Effect of Temperature on Fischer Tropsch Reactor 72
6. ECONOMIC ANALYSIS 74
6.1. Cost Estimation 74
6.1.1. Investment Costs 75
6.1.2. Operation Costs 76
6.1.3. Fixed Operation Costs 76
6.1.4. Variable Operation Costs 77
6.2. Profitability 78
6.2.1. Internal Rate of Return 78
6.2.2. Payback Period 79
7. SUMMARY AND DISCUSSION 80
8. CONCLUSIONS 82
9. RECOMMENDATION 83
REFERENCES 84

LIST OF TABLES

Table 1.Overview of Gasifier Types Items, furnace 16
Table 2. Fischer Tropsch Liquid Fuel 37
Table 3. Semi Emperical Fluid Dynamic Correlation 56
Table 4. Semi Emperical Fluid Dynamic Correlation 57
Table 5. Semi Emperical Fluid Dynamic Correction 57
Table 6.Component Model 64
Table 7.Equipment Specifications 65
Table 8. Aspen Plus Simulation Table Results 68
Table 9.Total Equipment Items Costs 74
Table 10. Total Investment Costs 75
Table 11. Total Operating Costs 76
Table 12. Fixed Operation Costs 76
Table 13. Variable Operation Costs 77
Table 14. Cost data for Feasibility Calculations 78
Table 15. Investment of Internal Rate of Return 79
Table 16. Payback Period of Investment 79

LIST OF FIGURES

Figure 1. Biomass gasification 9
Figure 2. Fixed bed gasifiers 12
Figure 3. Fluidized bed gasifiers 13
Figure 4. Foster Wheeler Energy Oy circulating fluidized bed gasifier 14
Figure 5. Mechanism of heat transfer 17

Figure 6. Heat transfer mechanism in a fluidized bed gasifier 20
Figure 7. Fischer Tropsch synthesis reactors; a. Slurry Bubble Column; b. Multitubular Trickle Bed Reactor; c.Circulating fluidized bed reactor; d. Fluidized bed reactor 31
Figure 8. Fischer Tropsch product distribution composition 36
Figure 9. Biomass Gasification with Fischer Tropsch synthetic reactor 38
Figure 10. Kinetic model for tar cracking 42
Figure 11. The conventional amine process 46
Figure 12. Pseudo equilibrium model 47
Figure 13. Gasification reaction steps 48
Figure 14. Kinetic model of Biomass Gasification 49
Figure 15. Derivation of Fluid Dynamic model 51
Figure 16 . Energy and material balance 62
Figure 17. Aspen plus Simulation process overview 67
Figure 18. Economic Analysis of Biomass Gasification via Fischer Tropsch synthesis 69
Figure 19. Effect of temperature on gasifier 70
Figure 20. Effect of temperature on heating value of syngas 71
Figure 21. Effect of temperature on water gas shift reactor 72
Figure 22. Effect of temperature on Fischer Tropsch synthetic reactor 73

LIST OF ABBREVIATIONS

DCOALIGT	Model gives the true Density of Coal or Biomass on a Dry basis
BTX	Benzene, Toluene, Xylenes
SNG	Synthesis Natural Gas
HLV	Lower Heating Value
HHV	Higher Heating Value
HCOALGEN	Nonconventional Component Enthalpy of Coal and Biomass
MIXCINC	Both Conventional and Nonconventional Solids are present.
UNIFAC	Property Method used for Vapor-Liquid Equilibrium Application

LIST OF SYMBOLS

Q	Heat duty	[kJ/hr]
m_{wood}	Mass flow rate of wood	[kg/hr]
C_p	Specific heat of gas, solid, steam and cluster	[kJ/kgK]
ΔT	Temperature difference	[K]
M	Molecular weight	[g/mole]
m_{ash}	Mass flow rate of ash	[kg/hr]
$F_{i,in}$	Molar flow rate of the feed	[kmol/hr]
$H_{i,in}$	Molar enthalpy of the feed	[kJ/mole K]
$F_{i,out}$	Molar flow rate of the product	[kmol/hr]
$H_{i,out}$	Molar enthalpy of product	[kJ/mole K]
R	Universal gas constant	[J/mole K]
V	Volume of the bed	[m^3/s]
A	Surface area of the bed wall	[m^2]
d_p	Diameter of gas particle	[m]
υ_g	Velocity of gas	[m/s]
μ	Dynamic viscosity of gas	[kg/ms]
ρ	Density of gas	[kg/m^3]
g	Acceleration due to gravity	[m/s^2]
HHV_{fuel}	Higher heating value of fuel	[MJ/kg]
LHV_{wood}	Lower heating value of wood	[MJ/kg]
h_{tot}	Total heat transfer coefficient	[W/m^2K]

$h_{cluster}$	Heat transfer coefficient due to conduction of cluster	[W/m^{2}K]
h_{rad}	Radiative heat transfer coefficient	[W/m^{2}K]
h_{con}	Convective heat transfer coefficient	[W/m^{2}K]
h_w	Conduction of heat transfer of gas layer	[W/m^{2}K]
k_g	Thermal conductivity of gas film	[W/mK]
k_s	Thermal conductivity of particle	[W/mK]
t_c	Mean residence time of cluster	[s]
σ	Stefan-Boltzmann constant	[kW/m^{2}K^4]

1. INTRODUCTION

The rising price of fossil fuels and tightening emission targets are making different energy sector actors more eager to invest in renewable energy sources. Utilization of biofuel via biomass gasification followed by Fischer Tropsch synthesis is of considerable interest because of the high quality fuels produced, which do not contain sulphur and are free of carbon dioxide. The process has high investment costs and his thus been considered technically and economically unfeasible [1].

The main reason for current interest in Fischer Tropsch synthesis for biofuel production is to reduce the emission of greenhouse gases, such as carbon dioxide. Furthermore, greater use indigenous biofuels will mean that countries are less dependent on imported fuels. For economic and logistic reasons, energy conversion should be made on a large scale [2].

Consequently, special attention is being addressed to the circulating fluidized bed reactor, because of its flexibility with respect to feedstock, such as woody biomass, high combustion efficiency, and longer residence time during operation [3].

Much research has been conducted into small scale biofuel production. Recent developments in advance Fischer Tropsch synthesis technology have greatly advanced framework for biomass utilization in Finland. This includes the development of energy efficient and low cost synthesis catalysts, improvements to the reaction process at large scales, and related process integration on the basis of a systematic development of the Fischer Tropsch reaction. The wood industry company, Stora Enso, and the energy company, Neste Oil have started programmes aiming to utilize wood biomass in large scale production at Varkaus [4].

The purpose of this Master's thesis is to simulate the Fischer Tropsch synthesis process in biofuel production using Aspen Plus to perform rigorous material and energy balances. The results of this simulation are used to carry out approximately economic and technical feasibility evaluation of the process, and to estimate the overall cost of energy production in large scale plants.

Biomass integrated gasification followed by Fischer Tropsch synthesis can become economically viable when crude oil price levels rise substantially, or when the environmental benefits of green Fischer Tropsch diesel are valued. Green Fischer Tropsch biodiesel is currently about 40% to 50% more expensive than biomass derived methanol or hydrogen, but it has clear advantage with respect to applicability to the existing infrastructure and car technology [5].

First generation biofuels have been produced from sugars and fats, utilizing either fermentation into alcohols or esterification into diesel oil. However, those techniques are not beneficial in the long term. Production of biofuel from woody biomass materials is a much more attractive option.

1.1. BACKGROUND

Fischer Tropsch synthesis was discovered in Germany in the beginning of the twentieth century, though due to its high costs it was only implemented on a large scale in South Africa, a result of the prevailing political situation and associated trading issues. Recently, it has become an attractive option for the energy sector, particularly in the context of conversion of natural gas to liquid transportation fuel [6].

The main driver for this interest in gas to liquid fuel conversion has been the increased availability of natural gas in locations, where no market exists, especially in the Asian-Pacific region. Natural gas, coal and biomass can be converted to carbon monoxide and hydrogen via existing modern technology. Important for Fischer Tropsch synthetic gas is the strong exothermic reaction. The reaction takes place in three phase systems, for instance in a gas phase, liquid phase and solid catalyst.

The amount of syngas and product molecules that transfer between the phases is quite large. Therefore, great demands are placed on the effectiveness of interfacial heat and mass transfer in Fischer Tropsch systems. The selection of the Fischer Tropsch reactor has some limitations based on fundamental principles [6].

The Fischer Tropsch reactor is operated at high temperature and moderate pressure. The reactor is operated typically at 250 ^{o}C and the pressure is somewhere between 40- 60 bar, which is higher compared with the biomass gasifier needed upstream.

1.2. GOALS

The main goal of the Master's Thesis is to investigate the feasibility study of integrated biomass gasification via a Fischer Tropsch system concept, and to estimate production costs of the feedstock in large scale production in which the Fischer Tropsch off gas, carbon monoxide and hydrogen, are completely purged to a gas turbine for electricity production. To achieve the above- mentioned goal, the Aspen ^{plus} Software Simulation program is implemented for the investigation.

2. BIOMASS GASIFICATION

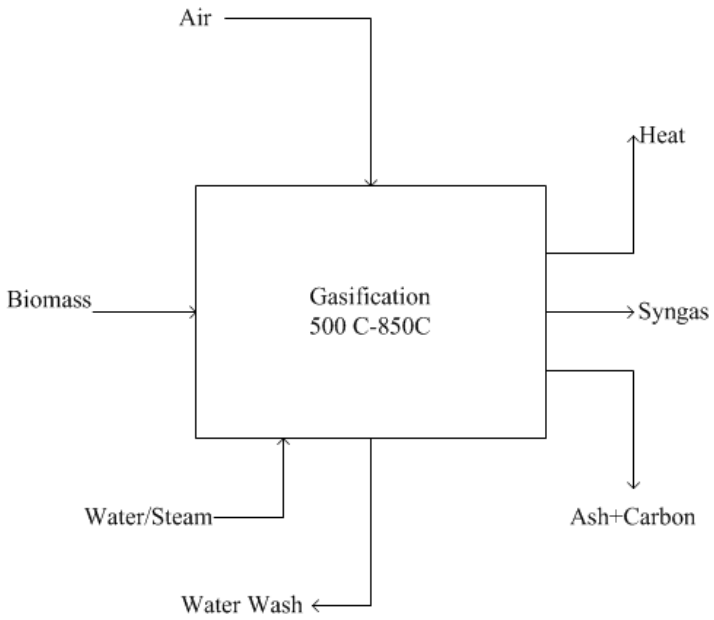

Figure 1. Biomass gasification

Global climate change together with increasing energy prices and depleting fossil resources have provoked major interest in renewable forms of energy. Gasification of biomass offers an efficient way to utilize renewable carbonaceous feedstock and therefore, has significant commercial and environmental potential in the production of green chemicals, synthetic fuels and electricity [7].

Gasification occurs when oxygen or air and steam or water is reacted at high temperature with available carbon in biomass or other carbonaceous material in a gasifier. The syngas produced can be combusted in an engine or gas turbine to generate electricity and heat. More recently, syngas has been considered a candidate fuel for fuel cell applications. Stoichiometric combustion occurs when all the carbon in the fuel is converted to carbon dioxide and there is no excess of oxygen left over.

The basic principle of gasification is to supply less oxidant than would be required for stoichiometric combustion of the solid fuel, and as a result, chemical reactions produce a mixture of carbon monoxide and hydrogen, both of which are combustible[8].

The energy value of gaseous fuel is typically 70% of the chemical heating value of the original solid fuel. The syngas temperature will be substantially higher than the original solid fuel due to the gasification process. Gasification can be divided into three parts. The first part is pyrolysis, which is also called devolatilization or, thermal decomposition. The second part is char gasification and the third part is partial char combustion. [9].

Solid pyrolysis and char conversion are used for gasification and combustion. Partial combustion is necessary because it supplies heat by the endothermic gasification reaction. Likewise, pyrolysis occurs in a temperature range between 450 ^{o}C to 800 ^{o}C and produces char, carbon monoxide, hydrogen, nitrogen, methane, carbon dioxide, water, tars and hydrocarbons.

Tars are extremely undesirable because they cause a loss of efficiency and degrade downstream plant equipment. However, if the temperature is high enough, some tars will be cracked to form hydrogen, carbon monoxide, carbon dioxide. The products of pyrolysis are then used in the gasification and combustion reactions.

The main objective of gasification is to maximize the yield of gaseous products and to minimize the amount of condensable hydrocarbons and unreacted char. The composition of the product gas depends on the types of process feeds, their ratios, process parameters, and the type of gasification reactor used.

2.1. Small Scale Gasifiers

At the end of the 80s and the beginning of the 90s, in Europe, small scale gasification received great support, e.g, many downdraft and updraft fixed bed gasifiers with capacities of less than a 100KW_{th} and a few >10 MW_{th}, facilities were developed and tested for small power and heat generation using diesel or gas engines [10].

Traditional fixed bed gasifiers are suitable only for feedstock which has high enough bulk density to guarantee stable fuel flow. Both updraft and downdraft fixed bed gasifiers have been developed and used in Finland. In downdraft gasifiers, the steam and oxidant are fed directly to the gasifier with fresh biomass. However, in the updraft gasifier, steam and oxygen contact with char.

Pyrolysis and combustion occur simultaneously. Tars are gasified to CO, CO_2 and H_2, and then the hot gases are swept downward over the remaining char to yield a relatively hydrocarbon free, low energy gas at the gasifier outlet. Combustion occurs at the base of the gasifier, and slower gasification reactions take place above the combustion. In the top areas, the biomass is devolatilized to produce a synthesis gas containing substantial quantities of hydrocarbons.

The most well known fixed bed gasifier operated with a range of biofuel is the `Bioneer` gasifier. The `Bioneer` gasifier has been in successful commercial operation in Finland and Sweden [11].

The critical demands of small scale gasifiers on fuel quality make it more expensive, for example, pellets must often be used, and small scale gasifiers have high operation costs, in part because of the need for effective gas cleaning to meet strict EU emission standards [10]. Figure 2 presents traditional fixed bed downdraft and updraft gasifiers.

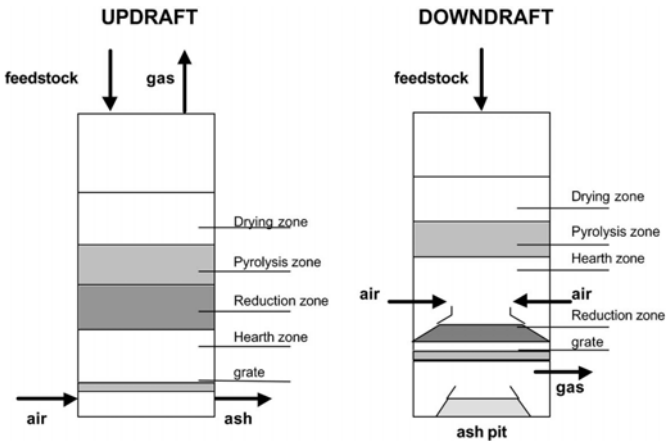

Figure 2. Fixed bed gasifiers [12]

2.2. Large Scale Gasifiers

Fluidized bed gasifiers are known for their fuel flexibility, i.e. capability to use different types of fuels, and their high conversion efficiency and longer residence time where a circulating fluidized bed or bubbling fluidized bed is used [13].

A single bubbling fluidized bed cannot achieve high solid conversion due to back mixing of solids and particle entrainment. In fluidized bed gasifiers, when a gas is passed upwards through a bed of particles, the degree of disturbance is determined by the velocity of the gas at low velocities, and there is little particle movement.

As the velocity increases the individual particles are gradually forced upwards until they reach the point at which they remain suspended in the gas stream. Consequently, increase in gas velocity causes turbulence, with rapid mixing of the particle [14]. Fluidized bed combustion of coal and biomass fuels uses a constant stream of air in sup or sub stoichiometric ratios during the combustion or gasification process, and creates important turbulence.

The beds of the particles are initially heated by a start- up fuel, mostly natural gas, after which the solid fuel is continuously fed to the bed and as a result, the fuel ignites and releases heat, which allows for the start-up fuel feed to be shut down.

Mixing of the particles encourages complete combustion and allows a constant temperature to be maintained during conversion. Part of the ash accumulates in the bed. When coal is used, these ash particles together with the sorbent material for sulfur capture will form the bulk of the particles. For biomass a fuel, which contains much less ash, the bed material mainly consists of sand.

Ash from fuel conversion and bed material is drawn from the bed at regular intervals and replaced when necessary to maintain the bed at a correct level and to maintain required bed properties [14], as can be seen in Figure 3.

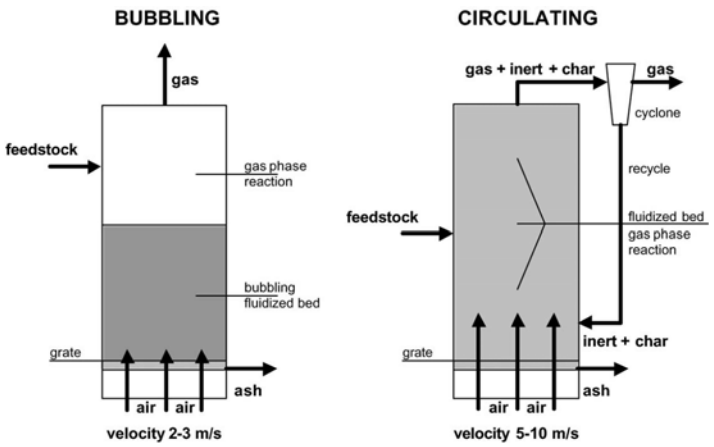

Figure 3. Fluidized bed gasifiers [12]

The first commercial circulating fluidized bed gasifier was developed by A. Ahlstrom CO, currently operating as Foster Wheeler Energia Oy in Finland in the 1980s [15]. Since then, similar gasifier plants having the same basic technology have been installed in Sweden and Portugal.

These gasifiers produce lime kiln fuel from bark and waste wood [16, 17]. Götaverken currently operating as Metso Power built one to Sweden that is still operating.

Today, biofuels are converted in the gasifier at atmospheric pressure and the temperature is about 850 ^{o}C. The hot fuel gas flowing through the cyclone is slightly cooled down in the air preheater before it is taken out from the main gasifier. Simultaneously, the gasification air is heated up in the air preheater before it is fed into the gasifier. The start-up fuel gas is led directly to the gasifier through to the two burners, which are located below the biomass feed points.

Therefore, wet woody biomass fuels and clean waste derived feedstock can only be utilized through a circulating fluidized bed [17]. Figure 4 presents a circulating fluidized bed.

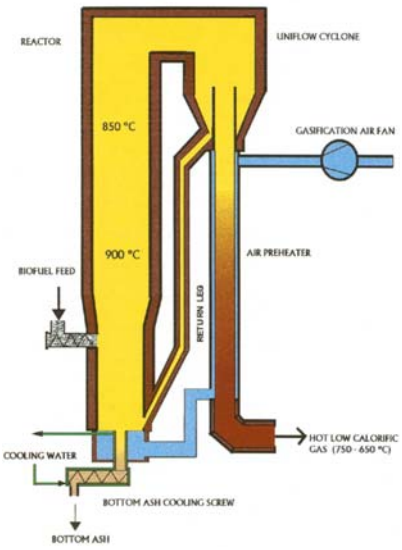

Figure 4. Foster Wheeler Energy Oy circulating fluidized bed gasifier [17]

In the CFB gasification process, large particles of the biomass ash can pass, together with the product gas, into the final use. If waste fuels are used they often contain high amounts of chlorine and alkali metals or aluminum, which have a tendency to cause severe corrosion and fouling problems in the gasifier [18].

Fortunately, one way of controlling corrosion and fouling in the gasifier is to lower the temperature and increase the pressure during the operation. The higher the temperature the higher carbon conversion, lowering temperature produces more residues as un-gasified char.

2.3. Advantages of Circulating Fluidized Bed Gasifiers

As mentioned previously, during industrial operation, fluidized beds have both desirable and undesirable characteristics. Circulating fluidized bed gasifiers have a number of unique qualities that make them attractive in energy production [3].

First of all, circulating fluidized beds are more flexible and a wide range of fuels can be used. The carbon conversion of a circulating fluidizing bed is typically 90% to 95% and the cold gas efficiency typically 75%. The higher carbon conversion rate is a result of better mixing of gas and solids, a high burning rate, and the longer combustion process of the fuels.

Circulating fluidized beds also have improved sulfur removal. The longer combustion process through the furnace gives a long reaction time for the limestone sorbent to react with sulfur dioxide. The average residence time of gas in the combustion process is about 3 to 4 seconds. Sulfur capture is dependent on the gasification temperature, around 780 ^{o}C to 800 ^{o}C, and as such also dependent on the fuel used. If lime is used then the temperature mentioned is applicable. In low temperatures limestone doe not convert to lime. Table 1 gives an overview of gasifier types

Table 1.Overview of Gasifier Types [3] Items, furnace

Iterms	Stocker Gasifier	BFB Gasifier	CFB Gasifier	PC Gasifier
Height of bed [m]	0,2	1-2	15-40	27-45
Superficial velocity [m/s]	1,2	1,5-2,5	4-8	4-6
Excess air %	20 -30	20 -25	10-20	15-30
Heat release [MW/m^2]	0,5 -1,5	0,5 -1,5	3 -5	4 -6
Coal, biomass size [mm]	32 -6	6 -0	6 - 0	< 0,001
Turndown ratio	4: 1	3:1	3 -4: 1	2: 1
Combustion efficiency %	85-90	90-96	95 -99	99
Nox emission ppm	400 -600	300 -400	50-200	400 -600
Sulphur capture in furnac %	none	80 -90	80 -90	small

2.4. Heat Transfer in a Circulating Fluidized Bed Gasifiers

This part presents a brief explanation of heat transfer in a circulating fluidized bed gasifier in order to understand the influence of design and operation parameters. Several models have been proposed to explain the behavior of heat transfer in a circulating fluidized bed gasifier and to predict heat coefficients. The process of heat transfer between the furnace wall and the bed includes contributions of radiation with convention from particles and the gas [19].

In general, the heat transfer between the furnace wall and the bed material in a fluidized bed occurs by particle convection, conduction, gas convection, and radiation in the case of temperatures greater than 500^{o}C [20].

The process of heat transfer in a circulating fluidized bed gasifier involves three mechanisms: conduction, convection and radiation. The contribution of each individual mechanism is not strictly additive, but for most practical application can be treated separately [21], as shown in Figure 5

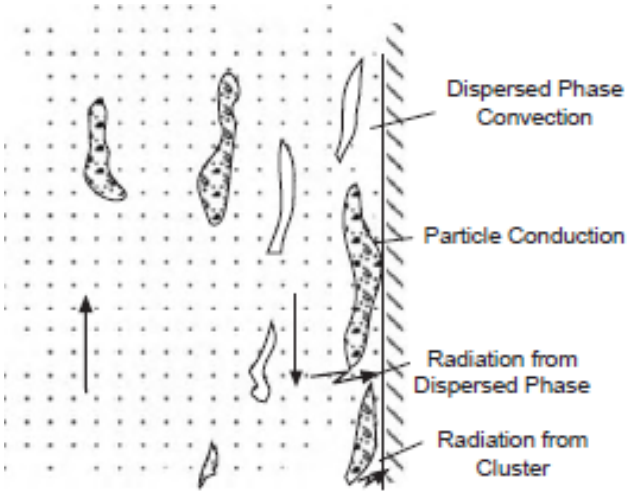

Figure 5. Mechanism of heat transfer [18]

The particle clusters travel down the wall a certain distance, disintegrate and reform periodically in the wall of the furnace, as shown in Figure 6. When the clusters slide over the wall, unsteady state heat conduction between the clusters and the wall takes place [22]. Therefore, the average heat transfer coefficient due to cluster conduction is given by the following Equation [23].

$$h_{cluster} = \left[\frac{4k_c(\rho c)_c}{\pi t_c} \right]^{0,5} \quad (1)$$

Where

$h_{cluster}$	Heat transfer coefficient due to conduction into cluster, W/m^{2}K
k_c	Thermal conductivity of gas film and cluster, W/m.K
$(\rho c)_c$	Density of cluster in the dilute section, kg/m^3
t_c	Mean residence time of cluster, s
π	Pi (constant≈3.14)

The overall total heat transfer coefficient may be expressed as a function of friction, which is the average fraction of the wall covered by clusters. The total heat transfer coefficients inside the circulating fluidized bed gasifier can be presented as in Equation 2[21].

$$h_{tot} = f(h_{con} + h_{rad})cluster + (1 - f)(h_{con} + h_{rad})dilute \qquad (2)$$

Where

h_{tot} Total heat transfer coefficient, W/m^2.K

f Fraction of wall covered by cluster, [-]

h_{con} Convective heat transfer coefficient, W/m^2.K

h_{rad} Radiative heat transfer coefficient, W/m^2.K

The particle clusters are major heat carriers between the core and the wall of a circulating fluidized bed. Consequently, a higher concentration of particles results in higher heat transfer. However, the contact time and contact area between the particles and the wall is small. Therefore, direct heat transfer from the particles to the wall through the point of contact is negligible.

Consequently, the majority of the heat is transferred through conduction across the gas gap residing between the clusters and the wall. The thermal conductivity of the gas, thus, greatly influences the heat transfer between the gas particle suspension and the wall.

The gas gap is often modeled as a particle free gap, the thickness of which decreases with an increase in the local suspension density at the wall. Since the particle volume fraction at the wall is proportional to that in the core, the cross section average suspension density represents the condition at the wall, which in turn affects the heat transfer through the particle coverage of the wall.

The thermal conductivity of a cluster can be calculated from an equation developed for heat transfer [24, 25].

$$\frac{k_c}{k_g} = 1 + \frac{M}{N} \tag{3}$$

The dimensionless (M) and (N) are defined as follows

$$M = (1-\varepsilon_c)\left(1 - \frac{k_g}{k_s}\right) \tag{4}$$

$$N = \left(\frac{k_s}{k_g}\right) + 0{,}28\varepsilon_c^{\,0.63\left(\frac{k_g}{k_s}\right)^{0{,}18}} \tag{5}$$

Where

ε_c Voidage in the cluster, [-]

k_g Thermal conductivity of gas film, W/m.K

k_s Thermal conductivity of particle, W/m.K

Therefore, the specific heat of a cluster can be calculated as a lumped property. The following formula has been presented by [19].

$$(\rho c)_c = (1-\varepsilon_c)\rho_p C_p + \varepsilon_c \rho_g C_g \tag{6}$$

The dimensionless ε_c is defined as follows, presented by [26] in the form of the following equation

$$\varepsilon_c = 1 - C_{sf} \tag{7}$$

Furthermore, the dimensionless C_{sf} can be calculated in the form [27].

$$C_{sf} = 1{,}23\left(1-\varepsilon_{avg}\right)^{0{,}54} \tag{8}$$

Where

$(\rho c)_c$ Density of cluster in the dilute section, kg/m^3

C_p Specific heat of cluster, solid, steam and gas, kJ/kgK

C_{sf} Cluster solid fraction, [-]

ε_{avg} Cross sectional average bed voidage, [-]

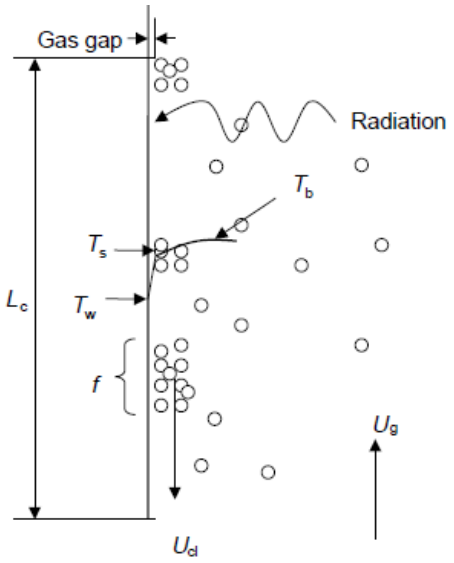

Figure 6. Heat transfer mechanism in a fluidized bed gasifier [21]

There is a temperature distribution in the horizontal section of the riser, as shown in Figure 6. Within the gas film, the temperature varies linearly from the wall to the surface. After contact with a wall surface, a cluster sweeps down the wall.

It initially accelerates to a steady velocity and then decelerates in the vertical direction before moving away from the wall.

Golriz [28], presents experimental results on radial temperature distribution in a circulating fluidized bed. The data were generalized in the form of Equation 9 by [29].

$$T_s = T_w + 1{,}29\left(\frac{\rho_s}{\rho_p}\right)^{0.13}\left(T_b - T_w\right) \tag{9}$$

Where

T_s	Solids temperature near the surface, K
T_w	Average wall temperature, K
T_b	Bed temperature, K
ρ_{savg}	Average suspension density, kg/m^3
ρ_p	Density of particle, kg/m^3

Therefore, it can be assumed that a cluster travels on the wall with average velocity over a characteristics length and then returns to the core, as shown in Figure 6. The residence time for each cluster at the wall surface can be expressed approximated by the following formula.

$$t_c = \frac{L_c}{U_{cl}} \tag{10}$$

Where

t_c	Residence time of cluster on wall, s
L_c	Characteristic length, m
U_{cl}	Velocity of cluster, m/s

Consequently, the cluster velocity can be estimated by the following correlation proposed by Noymer and Glicksmann [30].

$$U_{cl} = {}^{0,75}\sqrt{\frac{\rho_p}{\rho_g} g d_p} \tag{11}$$

Where

U_{cl} Velocity of cluster, m/s

ρ_p Density of particle, kg/m^3

ρ_g Density of gas, kg/m^3

d_p Diameter of gas particle, m

g Acceleration due to gravity, [9,81m/s^2]

A formula to calculate characteristic length is presented by [31].

$$L_c = 0{,}0178\left(\rho_{sus}\right)^{0,596} \tag{12}$$

Where

L_c Characteristic length, m

ρ_{sus} Suspension density, kg/m^3

According to Equation 2, heat conduction occurs across the thin gas layer between the cluster and the wall. The heat transfer coefficient due to that conduction through the gas layer is given as

$$h_w = \frac{k_g}{\delta d_p} \tag{13}$$

Where

h_w Conduction heat transfer coefficient of gas layer, W/m^{2}K

k_g Thermal conductivity of gas film, W/m.K

δ Non-dimensional gas layer thickness, wall and cluster, [-]

d_p Diameter of particle, m

The dimensionless δ is the gas layer thickness between the wall and the cluster and can be calculated using an expression given by [27] in the form of Equation 14.

$$\delta = 0{,}0282\left(1-\varepsilon_{avg}\right)^{-0{,}59} \tag{14}$$

Where

δ Non-dimensional gas layer thickness, wall and cluster, [-]

ε_{avg} Cross sectional average bed voidage, [-]

Therefore, by assuming that contact resistance and transient conduction through a cluster of particles act independently in series, the cluster convective heat transfer coefficient is given in the form of Equation 15.

$$h_{con} = \left[\frac{1}{h_{cluster}} + \frac{1}{h_w}\right]^{-1} = \frac{1}{\left[\frac{\pi t_c}{4k_c(\rho c)_c}\right]^{-0{,}5} + \frac{\delta d_p}{k_g}} \tag{15}$$

Where

h_{con} Convective heat transfer coefficient due to clusters, W/m^{2}K

$h_{cluster}$ Heat transfer coefficient due to conduction into cluster, W/m^{2}K

h_w Conduction heat transfer coefficient of gas layer, W/m^{2}K

The radiation of heat transfer from the cluster to the wall is considered as two parallel plates. Thus, the cluster radiation component of the heat transfer coefficient is estimated in the form of Equation 16 [32].

$$h_{cluster} = \frac{\sigma\left(T_s^4 - T_w^4\right)}{\left(\frac{1}{e_c} + \frac{1}{e_w} - 1\right)\left(T_s - T_w\right)} \tag{16}$$

Consequently, the radiation between the suspension dilute phase and the bare wall can be estimated from the usual expression for a parallel surface [33].

$$h_{rad} = \frac{\sigma\left(T_b^4 - T_w^4\right)}{\left(\frac{1}{e_d} + \frac{1}{e_w} - 1\right)\left(T_b - T_w\right)} \tag{17}$$

Where

$h_{cluster}$ Heat transfer coefficient due to conduction into cluster, W/m^{2}K

h_{rad} Radiative heat transfer coefficient, W/m^{2}K

σ Stefan-Boltzmann constant, kW/m^2.K^4

e_c Emissivity of cluster, [-]

e_w Emissivity of wall, [-]

T_s Cluster layer temperature, K

T_w Heat transfer on wall, K

The cluster emissivity can be calculated according to the formula presented by [32].

$$e_c = 0{,}5\left(1 + e_p\right) \tag{18}$$

Where

e_c Emissivity of cluster, [-]

e_p Emissivity of particle, [-]

The non-dimensional (e_d) can calculated in the form presented by [34].

$$e_d = \left[e_g + (1 - e_g)e_{pc}\right] \tag{19}$$

Where

e_d Emissivity of dispersed phase, [-]

e_g Emissivity of gas, [-]

e_{pc} Emissivity of particle cloud, [-]

Consequently, the non-dimension (e_{pc}) can be calculated in the form

$$e_{pc} = \left[1 - \exp\left(-\frac{1{,}5e_p F L_b}{d_p}\right)\right] \tag{20}$$

Where

F Volume fraction of solids in dilute phase, [-]

e_p Emissivity of particle surface, [-]

L_b Mean beam length, m

d_p Diameter of the particle, m

The dimension mean beam length (L_b) is calculated in the form

$$L_b = \frac{3{,}5V}{A} \tag{21}$$

Where

V	Volume of the bed, m^3
A	Surface area of wall, m^2

Similarly, the dispersed phase contains a small concentration of particles, which affects the heat transfer coefficient. Therefore, the expression for air flow through heat tubes was modified with a correction factor for particles [35].

$$h_d = 0{,}023 C_{pp} C_L C_t \frac{k_g}{D_b} \mathrm{Re}^{0{,}8} \mathrm{Pr}^{0{,}4} \tag{22}$$

Where

h_d	Convective heat transfer coefficient dilute phase, W/m^2K
C_{pp}	Presence of particle in the dilute phase, [-]
C_L	Correction factor for length, m
C_t	Correction factor for temperature difference, [-]
k_g	Thermal conductivity of gas, W/m^2K
D_b	Equivalent furnace diameter, m
Re	Reynolds number of gas and steam, [-]
Pr	Prandtl number of the gas and steam, [-]

The dimensionless (C_L), (C_t) and (Re) are defined as follows, and the correction factor for the tube length can be calculated according to the formula presented in [36].

$$C_L = 1 + F\left(\frac{D_d}{L}\right) \tag{23}$$

The correction factor for the temperature difference between a wall and medium can be calculated according to the formula presented by [35].

$$C_t = \left(\frac{T_b}{T_w}\right)^{0,5} \tag{24}$$

$$\mathrm{Re} = \frac{\rho v_g d_t}{\mu_g} \tag{25}$$

Where

ρ	Density of gas kg/m^3
v_g	Velocity of gas, m/s
d_t	Outer diameter for heat transfer, m
μ_g	Viscosity of gas, kg/ms

2.5. Entrained Flow Gasification

In the circulating fluidized bed plus tar cracker concept, the biomass is gasified and subsequently brought to a high temperature to destroy the tars and hydrocarbons. Alternatively, high temperatures may be established directly in the gasifier. In the latter concept an entrained flow gasifier can be applied via Fischer Tropsch synthesis [37].

Once raw material has been fed inside the gasifier, the feedstock is gasified with oxygen in a co-current flow. The temperatures are usually very high in comparison to fluidized beds, ranging from 1300 ^{o}C to 1500 ^{o}C. The high temperature cracks the tars thermally into lighter hydrocarbons and causes the ash to melt. The melted ash then has to be removed from the bottom of the gasifier in the form of slurry [38].

Due to the pre-treatment requirements and ash conditions inside the gasifier, entrained flow gasifiers usually need to be very large scale in order to be economic, thus posing challengers for commercialization of biomass applications, which are usually confined to a smaller scale because of biomass availability. The pre-treatment of biomass is a major operation in terms of equipment size, energy consumption and cost.

Examples of entrained flow gasifier manufacturers include Shell, Conoco-Phillips, Texaco and Future Energy (formerly Noell / Babcok Borsig Power). Unfortunately, high temperature entrained flow gasification technology for biomass does not yet exist commercially. It should be noted that current entrained flow gasifiers are not fuel flexible, a quality which is considered to be of vital importance for large scale plant operation [37].

2.6. Biomass pre-treatment

Biomass feedstocks are extremely varied in chemical composition and physical appearance. The moisture content, in particular, and ash composition can vary greatly. The presence of fuel-derived sulphur in the product gas is normally problematic for gasification process, but less so for biomass feedstocks than coal feedstocks.

Energy processes that use biomass as feedstock are usually sensitive to changes in the feedstock quality. For this reason, several kinds of pre-treatment technologies have been developed to make biomass more homogeneous in terms of size, moisture content and density.

For the purpose of synthesis gas production, the moisture content of the feedstocks must usually be dried down to 30-15%. Drying to low moisture content is however problematic and has not yet been optimized for biomass conversion processes.

2.7. Drying of Biomass

Drying is the most important pretreatment operation, and very necessary for high cold gas efficiency at the gasification stage [39]. Drying usually reduces the moisture content from 10 to 15%. Drying can either be done with flue gas or with steam. Based on literature studies, a significant amount of low quality steam is generated in the Fischer Tropsch process, and steam drying is generally preferable [40].

At present, most dryers commonly used at bioenergy plants are direct rotary dryers, but the use of steam drying techniques is increasing because of easy integration to existing systems and the lack of gaseous emissions. On the other hand, steam dryers produce aqueous effluents that often need treatment [41].

Energy density upgrading technologies include both thermo-mechanical and thermo-chemical means, like pelletization, torrefaction and pyrolysis. Steam drying has very low emissions and is usually safer with respect to the risks of dust explosion. The usage of flue gas is, however, the cheapest way of drying the feedstock.

3. FISCHER –TROPSCH SYNTHESIS

Fischer Tropsch synthesis was invented by the German scientists, Franz Fischer and Hans Tropsch at the Kaiser Wilhelm Institute for coal research in Mulheim, Germany in the 1920s [2]. Fischer Tropsch synthesis is one of the technology alternatives being used by SASOL in, South Africa, and Shell in Malaysia, since the 1970s oil crisis, to obtain liquid fuels from syngas [42].

Synthetic gas is derived from carbon sources such as coal, peat, biomass and natural gas and converted into hydrocarbons and oxygenates. Recently, Fischer Tropsch synthesis has attracted increasing interest as an option for production of clean transportation fuel and chemical feedstocks [43]. Fischer Tropsch synthesis gas is composed of a complex multi component mixture of hydrocarbon products [44, 45].

Fischer Tropsch products vary depending on the feed composition, the type of reactors, the catalyst employed, and operating conditions such as temperature, pressure and velocity. Use of the Fischer Tropsch process has received much attention because its hydrocarbon products are ultra clean fuels due to the nature of the synthesis process.

Fischer Tropsch synthesis kinetics has been extensively studied, and many attempts have been made to define rate equations describing the Fischer Tropsch reactions [45, 46]. In most cases, the hydrocarbon products were lumped according to the carbon number of hydrocarbon molecules with an ideal Anderson Shulz Flory distribution.

A few kinetic models have been developed based on the detailed mechanism of the Langmuir Hinshelwood Hougen Watson model [46, 47]. Unfortunately, few of them can predict overall reaction rates as well as product distribution. Wang et al., 2003 have proposed a model for a Fe, Cu and K catalyst in a fixed bed reactor [46].

The development of Fischer Tropsch reactors has been reviewed by several researchers, including [6, 48, 49]. Both gas phase and liquid phase reactors are currently in use commercially for the Fischer Tropsch synthesis process. The selectivity is either toward wax for the low temperature Fischer Tropsch process or gasoline for the high temperature Fischer Tropsch process. In some cases, a combination of both reactors can be used to meet the need for flexibility in response to market demand.

The low temperature reactors are either fixed -bed type or slurry type, whereas fluidized bed reactors, fixed bed or circulating bed reactors can be used for the high temperature Fischer Tropsch process. It should be noted that a large number of downstream operations are needed for both the high temperature and low temperature Fischer Tropsch process before the final product is ready.

The focus of Fischer Tropsch research has recently shifted to product distribution, with the aim of maximizing the yield of gasoline, diesel and commercially-valuable chemicals. Most of these efforts are on the catalyst level [50, 51]. Although some researchers are trying to change the product distributions on a micro scale by changing the reactor or process design [52]. Figure 7 presents Fischer Tropsch synthesis reactors.

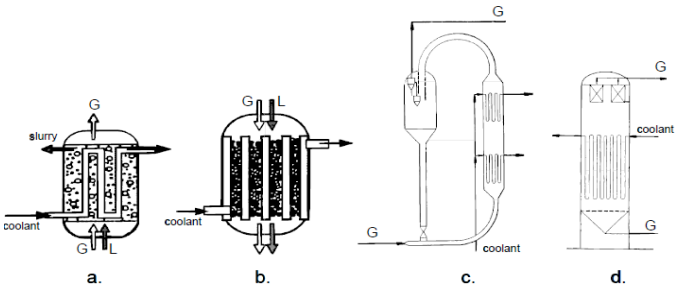

Figure 7. Fischer Tropsch synthesis reactors; a. Slurry Bubble Column; b. Multitubular Trickle Bed Reactor; c.Circulating fluidized bed reactor; d. Fluidized bed reactor[53].

3.1.1. Synthesis

One mole of carbon monoxide reacts with two moles of hydrogen to form mainly a paraffin straight chain hydrocarbon [54]. The process can be operated in a temperature range from 200 ^{o}C to 250 ^{o}C and at pressure levels between 25 to 60 bars.

Through the exothermic reaction process, the estimated loss can be 18% to 20% for all carbon monoxide and hydrogen converted. Adding a maximum of 1% to 2% shift losses, the energy loss due to the reaction would be around 20%. Other losses at the end of the process might make an overall efficiency loss of 25% but these losses are not related to the exothermic reaction.

The LHHW kinetic model has been much considered by many researchers due to its ability to predict the reaction rate through a Fischer Tropsch reactor. Equation 26 presents the LHHW input kinetic model.

$$r = \frac{(\text{kinetic factor})(\text{driving force expression})}{(\text{adsorption expression})} \tag{26}$$

The dimensionless (kinetic factor), (driving force expression) and (adsorption term) are defined as follows:

$$\text{Kinetic factor if } T_o \text{ is specified } = k(T/T_o)^n e^{-(E/R)[1/T-1/T_o]} \tag{27}$$

$$\text{Kinetic factor if } T_o \text{ is not specified } = kT^n e^{-E/RT} \tag{28}$$

$$\text{Driving force expression } = \mathrm{K}_1\left(\prod C_i^{v_i}\right) - K_2\left(\prod C_j^{v_i}\right) \tag{29}$$

$$\text{Adsorption expression} = \left[\sum K_i\left(\prod C_j^{v_i}\right)\right]^m \tag{30}$$

Where

r	Rate of reaction, kgmole/s-m^3
k	Pre exponential factor, kgmole/s
T	Temperature, K
T_o	Reference temperature, K
n	Temperature exponent, [-]
E	Activate energy, kJ/mol
R	Universal gas constant, 8.314J/kmol.K
C	Component concentration, kmol/m^3
m	Adsorption expression exponent
K_1, K_2, K_i	Equilibrium constants, [-]
v	Concentration exponent, m^3/s
i, j	Component index, [-]

The main reactions of the Fischer Tropsch synthesis equations are shown in equations 31-38 [55].

Main reactions

Paraffins: $nCO + (2n+1)H_2 \rightarrow C_nH_{2n+2} + nH_2O$ (31)

Olefins: $nCO + 2nH_2 \rightarrow C_nH_{2n} + nH_2$ (32)

Water gas shift reaction: $CO + H_2O \rightarrow CO_2 + H_2$ (33)

Side reactions

Alcohol: $nCO + 2nH_2 \rightarrow C_nH_{2n} +_2 O + (n-1)H_2O$ (34)

Boudouard reaction: $2CO \rightarrow C + CO_2$ (35)

Catalyst modification

Catalyst oxidation/reduction: $a * MxOy + yH_2 \leftrightarrow yH_2O + xM$ (36)

$b * MxOy + yCO \leftrightarrow yCO_2 + xM$ (37)

Bulk carbide formation: $yC + xM \leftrightarrow MxCy$ (38)

3.1.2. Catalysts

Several types of catalysts can be used for Fischer Tropsch synthesis. The most important catalysts are Fe and Co. In general, Co catalysts react more in hydrogenation, producing less unsaturated hydrocarbons and alcohols compared to Fe catalysts [54]. Fe catalysts have higher tolerance for sulphur, and are cheaper, but produce more olefin products and alcohols.

Use of a cobalt catalyst is preferred due to its properties during the reaction. The Fischer Tropsch reaction consumes H2/CO in a molar ratio. Many kinetic models are available in the literature that can predict the Fischer Tropsch and water gas shift reaction rates [56].

3.1.3. Water Gas Shift Reaction

The water gas shift reaction is the conversion of carbon monoxide and steam to form hydrogen and carbon dioxide. The reaction can also be used to increase hydrogen concentration in the syngas.

According to the reaction 28 above, water gas shift does not involve net change in volume and is therefore only remotely affected by the operation pressure. The reaction is reversible, with the forward reaction being exothermic and thus favorable to low temperatures. Higher temperatures will increase the rate of the reaction but decrease the yield of hydrogen. Therefore, in order to achieve high yields at high rates of reaction, water gas shift is usually carried out at both high and low temperatures.

During the Fischer Tropsch reaction, α indicates the probability of given alkyl compounds forming paraffin and olefins or propagating to the next higher alkyl compounds. Alpha is dependent on the operating conditions as well as the nature of the catalyst [57].

The Anderson Schulz Flory polymerization is given in Equation 39. The linear Arrhenius relationship is usually expressed in logarithmic form with $\log(Wn/n)$ and n having slope $\log\alpha$ in the Fischer Tropsch distribution [58].

$$\log(Wn/n) = n\log\alpha + \log\left[\left((1-\alpha)^2/\alpha\right)\right] \tag{39}$$

Where

$\log(Wn/n)$	Logarithmic form, [-]
Wn	Weight fraction of the product, [-]
n	Carbon number, [-]
α	Growth probability of Fischer Tropsch, [-]

The reaction is based on the catalyst weight, and therefore, the rate constant can be found using the Arrhenius relation. As a result, α is influenced by temperature, pressure, feed gas composition and catalyst composition [42].

For example, the value of α increases with increase in the iron or cobalt catalyst, and increases in the order: $Li < Na < K < Pb$. At higher operating temperatures, the product distribution shift toward more hydrogenated and higher carbon number products decreases as the values of α become smaller

The effect of pressure and feed gas composition on α is not straight-forward because of the formation of carbon dioxide and water during the reaction, which complete with carbon monoxide and hydrogen for adsorption on the catalyst surface and change the chain growth probability such that it becomes more complicated.

3.1.4. Product Distribution

Fischer Tropsch product distribution from syngas potentially includes methane, propane, butane, methanol, ethanol, isobutanol, dimethyl ether, methyl acetate, dimethyl carbonate, gasoline, diesel and paraffin waxes. As can be seen from Figure 8, the lighter hydrocarbons, C_1 to C_2 can be used to generate the hydrogen utilized downstream to refine the heavier hydrocarbons.

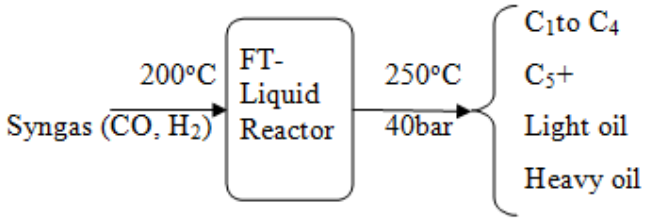

Figure 8. Fischer Tropsch product distribution composition [59]

The energy produced from Fischer Tropsch synthesis is 70% syngas, including C_1 to C_4, and 25% of the energy is released as heat. The remaining 5% of the energy is contained in the Fischer Tropsch off gases, i.e. unconverted syngas. C_1 and C_4 products can be used to generate electricity [2]. Table 2 shows differences in conversion efficiencies. It should be noted that the conversion efficiencies are strongly dependent on the α values of the catalysts.

Table 2. Fischer Tropsch Liquid Fuel [2]

Syngas Conversion (η_{CO+H_2})	FT products (η_{FT})	FT C_{5+} products (η_{C5+})	Hydro cracking to fuel (η_{Hydro})	Gas to fuel (η_{G+F})
0,95	0,80	0,95	0,98	0,71

Major changes in biofuel production are required to meet ambitious targets for renewable synthetic gas energy, and biofuel plants will require fuel flexibility and highly efficiency technology for optimum biomass utilization, as well as good availability of biomass [60].

Consequently, two possible approaches can be adopted. The first approach comprises scaling up of small-scale gasification technologies, which currently are mostly used for distributed heat and power production. The second approach is the development of novel technologies for large-scale biomass gasification.

4. PROCESS DESCRIPTIONS

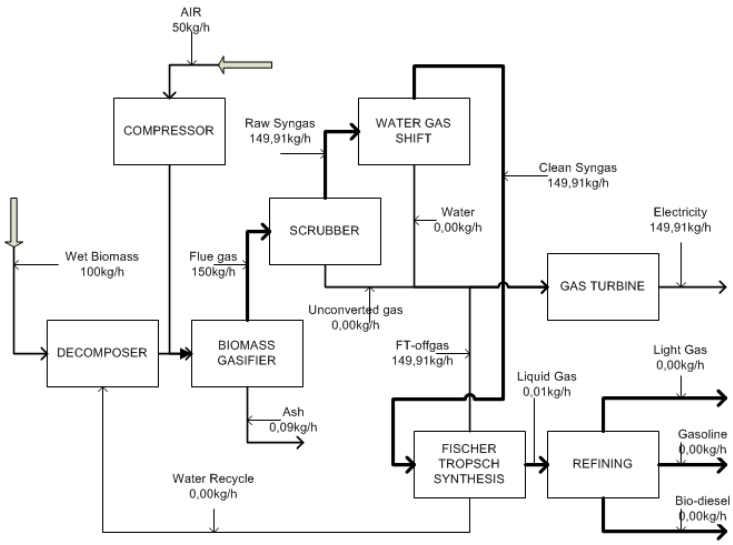

Figure 9. Biomass Gasification with Fischer Tropsch synthetic reactor

In biofuel production, several processes have to be completed before the final liquid fuel is clean enough. All tars and aromatic compounds must be purified. The Fischer Tropsch off gas, carbon monoxide and hydrogen are completely purged to a gas turbine for electricity production.

In order to clarify the process, the flow diagram in Figure 9 presents the simulated process diagrammatically. In the process, wet wood reacts with steam in a gasifier at a temperature of 850 ^{o}C and pressure of 1 bar. Solid waste product is removed from the cyclone as ash, and char is recycled back to the main gasifier.

The remaining products, inert gases from the gasifier, are cooled to 600 ^{o}C and pass into the wet gas scrubber, where the temperature increases to 1000 ^{o}C and the pressure drops to 0, 5 bars, and where tars and inorganic impurities are removed.

The clean syngas then moves upward as gas vapor from the wet gas scrubber to the water gas shift, while, tars and unconverted gas pass through a heat exchanger and are sent to the gas compressor.

A water gas shift reactor is used to increase the H2/CO ratio of the syngas. The main reaction in the water gas shift process is the conversion of carbon monoxide and water steam to carbon dioxide and hydrogen. The temperature and pressure of the exothermic water gas shift reactor are controlled at a temperature 400 ^{o}C and pressure of 1 bar to meet the requirements of the modeling application and so that the model satisfies the need for 95% conversion.

Heat exchangers are connected to control the reaction temperature and to generate saturated steam at 1 bar. The clean syngas is finally cooled to 300 ^{o}C and is then sent to the Fischer Tropsch synthetic reactor. In a similar way, in the Fischer Tropsch synthetic reactor, the temperature and pressure are increased to 250 ^{o}C and 25 bars. The outlet product from the Fischer Tropsch synthetic reactor contains offgas and light gases.

The off gases are separated and transferred to a second heat exchanger. Off gas, together with unconverted gases, is sent to the gas compressor, and then transferred from the gas compressor to the gas combustor reactor at high temperature and pressure, and finally sent to the gas turbine for electricity production.

Any remaining light gases from the Fischer Tropsch synthetic reactor are transferred through a refining reactor for production of fuels such as gasoline and biodiesel, and after dewatering the gases are separated and recycled back to the main DECOMP (RYield) reactor.

4.1. Tar Treatment Technologies

In addition to the main gas components, biomass derived product gas contains a variable amount of organic and inorganic impurities, as well as particulates. The organic impurities range from low to high molecular weight hydrocarbons. While the low weight hydrocarbons can be used as fuels in many applications, for example, in gas turbines, heavy hydrocarbons must be treated before end use.

Higher molecular weight hydrocarbons are normally referred to as “tars”. The precise definition of tars is not always clear and the term tar refers to many substances. Many definitions can be found in the literature [61]. Generally, tars can be considered to be heavy hydrocarbons that are difficult to treat by thermal, catalyst or physical processes.

Formation of tars begins at low temperature, from 400 ^{o}C to 600 ^{o}C, when cellulose and lignin molecule bonds are broken to form primary tars like laevoglucose, hydroxycetaldehyde and furfurals. When the temperature increases from 600 ^{o}C to 800 ^{o}C secondary tars are formed, such as phenolics and olephines. Tertiary tars, like aromatics, form when the temperature is 800 ^{o}C to 1000 ^{o}C [62].

The composition of tars depends on the transformation process and parameters such as temperature, residence time, oxygen, ratio, moisture content, composition and size of particle, as well as the nature of the material being gasified. Also on catalytic effects of e.g Na and K in the wood [63].

Han and Kim [64] have divided tar removal technologies into five groups: mechanical methods; self modification for selecting optional operation parameters for a gasifier or usage of a low tar gasifier; catalytic cracking; thermal cracking methods; and plasma methods.

The first three methods do not lead to removing a significant fraction of tar due to their applications. Thermal cracking seems, however, to be an interesting approach, provided that the temperature is high enough. Nevertheless, a drawback of this method is the decrease in the LHV of the syngas because the high temperature is reached by burning a part of the syngas itself [65].

In thermal cracking air is decreased and used as the oxidant because of the subsequent addition of nitrogen in the gasifier. The performance of the gas cleaning can be evaluated by the tars conversion, and tertiary tars are problematic because of their high dew point [66].

4.1.1. Thermal Cracking of Tars

In order to design effective tar cracking, kinetic model compounds have to be selected. In the case of gasification, the temperature can be higher than 600 ^{o}C. [67] Observed that tar cracking, which appears at temperatures higher than 600 ^{o}C in primary tars, might lead to phenol, naphthalene and benzene. Therefore, secondary tars may be partially cracked, while tertiary tar may not undergo cracking since they require higher temperature or the presence of a catalyst

In order to build a reaction pathway for the thermal cracking of tars, it is necessary to first define the model compounds. These model compounds have to be representative of the class of tars, i.e. secondary and primary tars. Toluene is a good example because it presents a stable aromatic structure found in tars formed in high temperature processes [68-70].

Naphthalene is very difficult to crack compared to other tertiary tars and is very often found in the gasification. For that reason, naphthalene is presented as a secondary class of tertiary tar. Benzene is not considered as tar based on the kinetic model presented by Fourcault [61].

Few data exist for thermal cracking that might demonstrate both the reaction pathway and the kinetic model involved in the thermal operation. Li and Suzuki listed possible reactions that might happen during thermal decomposition of tars [66].

$$\text{Thermal cracking: } pC_nH_x \rightarrow qC_mH_y + rH_2 \tag{40}$$

$$\text{Steam reforming: } C_nH_x + nH_2O \rightarrow (n + x/2)H_2 + nCO \tag{41}$$

$$\text{Dry reforming: } C_nH_x + nCO_2 \rightarrow (x/2)H_2 + 2nCO \tag{42}$$

$$\text{Carbon formation: } C_nH_x \rightarrow nC + (x/2)H_2 \tag{43}$$

Where

C_nH_x	Represents tar
C_mH_y	Represents hydrocarbons with smaller carbon number

As the thermal cracking products are known, the naphthalene and benzene reaction can be set up. A simple reaction scheme for tar cracking has been established by [61]. Soot is assimilated to solid carbon. The chemical reactions are as follows

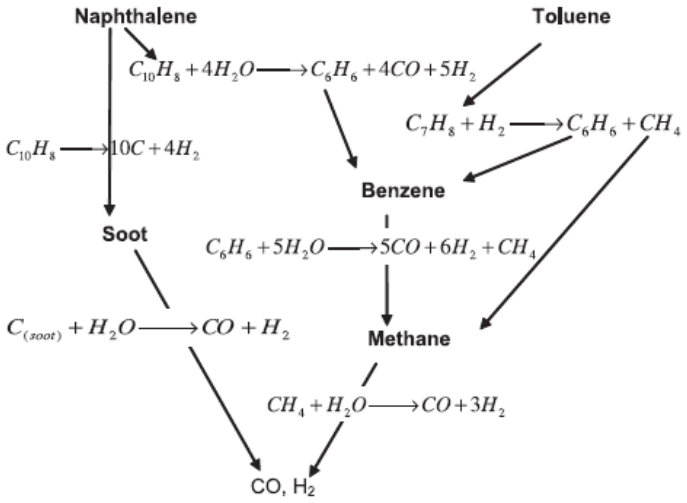

Figure 10. Kinetic model for tar cracking [61]

4.1.2. Physical Tars Removal

The secondary treatment consists of removal of tar in downstream operations based on physical methods such as scrubbers or catalytic strategies. Extensive research work related to both approaches has been done and it has been concluded that the necessary degree of reduction of tars cannot be achieved by means of only primary or secondary treatment. The quantities of products from tar decomposition can be of the order of 5000 ppm, and the desired product should minimize downstream fouling and coking. Therefore, tars removal is important to ensure economic and effective fuel gas utilization [71].

4.1.3. Catalytic Tars Removal

The most economical way for removing tars is to use catalytic cracking and to lower the molecular weight of the hydrocarbons, preferably to methane. Consequently, this catalytic tar removal is an important component in any catalytic hot gas clean up. For tar decomposition, methane is not a desirable product itself [72].

Catalytic tars removal has received much attention because tars can be cracked or reformed into gaseous components, increasing the overall efficiency of the gasification process [73]. The most widely researched approaches are based on dolomites, alkali metals, and nickel. Extensive research has been performed on dolomites since they are inexpensive, abundantly available, and show good catalytic activity [74].

Other catalyst materials have been investigated such as alkali metals. Alkali metals are usually added to the feed by dry mixing or wet impregnation methods. Although, they show good catalytic activity towards tars removal, several disadvantage exist. For instance, the alkali metal catalyst can lose its activity due to particle size agglomeration, and it volatilizes gases.

In addition, recovery of the catalyst material is very difficult since it is usually added along with the biomass. The overall process thus becomes more expensive because of costs associated with the separation of the alkali metals from char and ash, in addition to ash disposal issues.

For the above-mentioned reasons, the most widely investigated catalysts for tars removal are nickel supported catalysts. Nickel catalysts exhibit high activity toward steam and dry reforming, ensuring complete tar removal and increasing the hydrogen and carbon monoxide content of the fuel gases [75]. Catalysts for tar removal reactions can be used in the gasifier and in secondary catalytic reactors in which tars react with some of the permanent gases in the flue gas at temperatures inaccessible to the gasification reactor [76]

Hydro cracking the tars all the way to methane may be either desirable or undesirable depending on the end use of the biomass gas. If the gas is to be used for energetic purposes, then conversion into methane will increase the heating value of the gas. But if the gas is to be used for synthesis of methanol or ammonia, then methane is undesirable [77].

4.2. Cleaning of Syngas

Raw syngas produced in a gasifier is very hot and contains many impurities such as particulates, soot, and undesirable gas components like acidic gases. It also contains high amounts of carbon monoxide, which is not desirable for many downstream applications. Therefore, conditioning and cleaning of syngas is required for efficient use in various applications

The major components of syngas produced in a gasifier are carbon monoxide and hydrogen. Other gases such as carbon dioxide, hydrogen sulfide and carbon sulfur are also present, along with some char particles and ash. Of these components of syngas, hydrogen sulfide, carbon sulfur and carbon dioxide tend to be acidic gases.

These gases produce acidic solution after dissolving in water, which causes corrosion under the moist conditions in the gasifier. Carbon dioxide is also responsible for global warming. Thus, the removal of these gases from syngas is essential for reducing corrosion in the gasifier, as well as green house gas emissions to the atmosphere. Cleaning of syngas also includes the separation of char or soot particles along with acidic gases [78]

4.2.1. Particulate Cleaning

Char materials and ash can be removed from syngas in a two-stage water wash, consisting of a quench pipe and packed tower. In the quench pipe, about 95% of the carbon can be removed by direct water spray. In the scrubber, syngas is washed in counter current flow in two packed beds.[79]**.** As mentioned previously, the use of hot gas has many advantages for the cleaning of tars, ammonia, hydrogen sulfide and other byproducts from the raw syngas [80]

4.2.2. Acidic Gas Removal

The removal of carbon dioxide and hydrogen sulfide from natural gas is a process of substantial industrial important because of health and environmental problems, and to lower emissions [81]. The conventional gas sweetening process consists of absorption or stripping of carbon dioxide and hydrogen sulfide with aqueous amine solutions, 70% of the processes used for treating natural gas use absorption stripping [82].

Since acid gas removal from natural gas requires regeneration of alkanoamines, the energy requirement for the stripping will be much greater when the natural gas contains a high concentration of acid gases.

Extensive research has been performed on the conventional gas sweetening process with various alkanoamines solutions such as monoethanolamine (MEA), diethanolamine (DEA) and methyldiethanolamine (MDEA). MEA and DEA are very reactive and able to absorb acidic gases at a very fast reaction rate [83]. Figure 11 presents the conventional amine process for acidic gases removal.

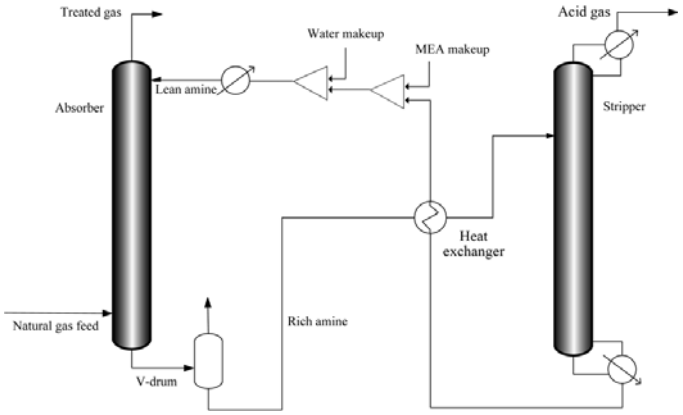

Figure 11. The conventional amine process [84]

5. MODELLING OF BIOMASS GASIFICATION

The aim of the modeling of biomass gasification in a fluidized bed gasifier is to construct a mathematical process description that can be used to predict reactor temperature and outlet concentration from inlet flows as well as operating conditions. Mathematical models of fluidized bed gasifiers are usually based on the kinetic rate or thermodynamic equilibrium [7].

The equilibrium model can only predict the end-reaction product distribution and cannot describe the instantaneous product distribution along with geometric dimensions [85]. Therefore, the equilibrium model does not seem to be very appropriate for the design of fluidized bed biomass gasifiers [86].

Nevertheless, the equilibrium model is simple and useful for estimations, and in order to improve this model, a pseudo equilibrium model or advanced model can be applied [87]. Figure 12 presents a pseudo equilibrium model

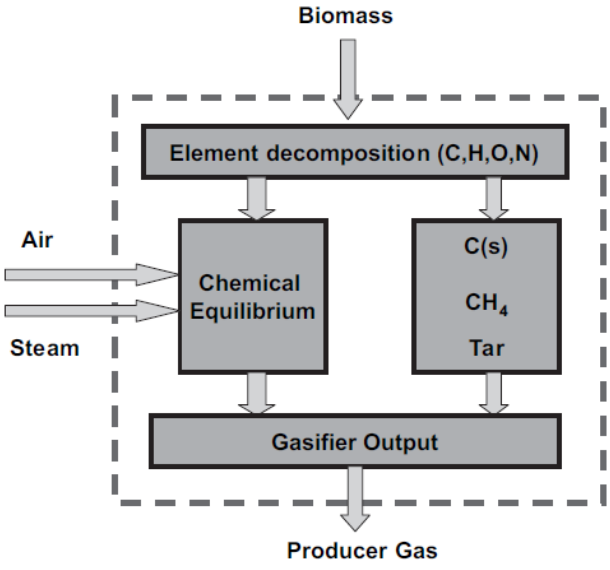

Figure 12. Pseudo equilibrium model [88]

For the mechanism of biomass pyrolysis and biomass gasification, the kinetic model can simulate the reaction condition at deferent times, which makes it suitable for reactor simplification design and evaluation of operation parameters [89].

The chemistry of biomass gasification is complex. Biomass gasification proceeds primarily via a two-step reaction, pyrolysis followed by char gasification. Pyrolysis is the decomposition of biomass raw materials by heat. This step, also known as devolatilization, is endothermic and produces 75% to 90% volatile materials in the form of gaseous and liquid hydrocarbon. The remaining material is non volatile material, having high carbon content, and is referred to as char. Figure 13 presents the gasification reaction steps [90].

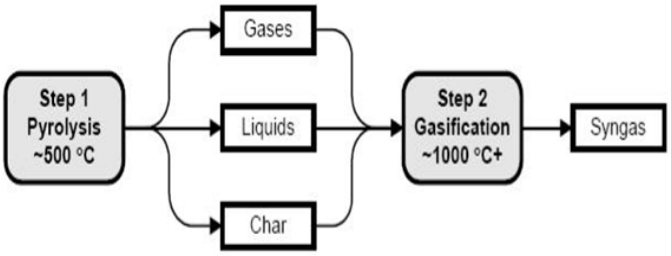

Figure 13. Gasification reaction steps [90]

Biomass pyrolysis is one the important processes of biomass gasification and quite a lot of work has been done on its mechanism and modeling [91]. As mentioned previously, biomass gasification is a complicated process which includes numerous chemical reactions such as drying, particle decomposition and devolatilation, oxidation and reduction reactions. Various products can be obtained from the reactions [92]. Figure 14 presents a kinetic model of biomass gasification [93].

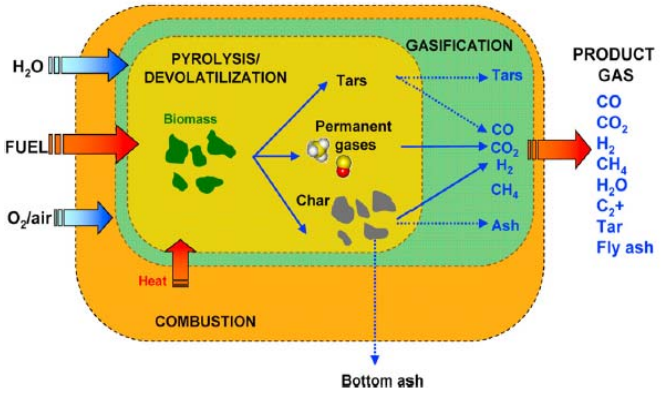

Figure 14. Kinetic model of Biomass Gasification [93]

In order to simply the model calculations, it is often considered better to ignore axial gaseous diffusion caused by the concentration of gas in the bubble phase and emulsion phase. This assumption is quite far from the actual conditions and causes errors in the calculation. Therefore, in order to reduce simulation error, the gaseous flow in a bubble and emulsion phase is considered to be plug-flow [89]. In the literature, modeling of biomass gasification in fluidized bed gasifiers is mostly one-dimensional and two-phase [94].

5.1. Model Mechanism

In general, modeling of biomass gasification in a fluidized bed is constructed based on three reaction steps. In the first step, the biomass particle decomposes quickly to form char, tar and gaseous products. Reactions between the gaseous products occur in the second step, and tar cracking and char gasification in the third step [93]. The following reactions occur.

$$C + O_2 \xrightarrow{k_o} CO_2 \qquad (44)$$

$$C + CO_2 \xrightarrow{k_1} 2CO \quad (45)$$

$$C + H_2O \xrightarrow{k_2} CO + H_2 \quad (46)$$

$$C + 2H_2 \xrightarrow{k_3} CH_4 \quad (47)$$

$$CO + H_2O \xrightarrow{k_4} CO_2 + H_2 \quad (48)$$

$$CO_2 + H_2 \xrightarrow{k_5} CO + H_2O \quad (49)$$

$$2CO + O_2 \xrightarrow{k_6} 2CO_2 \quad (50)$$

$$CH_4 + H_2O \xrightarrow{k_7} CO + 3H_2 \quad (51)$$

For the fluidized bed model shown in Figure 15, it is assumed that bubble and emulsion phases exist in the fluidized bed, and there is gas exchange between these two phases. The axial diffusion is considered in the bubble phase and emulsion phase. Therefore, the assumptions of this model are as follows: the fluidized bed reactor consists of two phase bubble and emulsion phases, which are homogeneously distributed; the voidage of the emulsion phase remains constant; and the bubble diameter, which can be expressed as an equivalent bubble diameter, and the gas flow in the two phases is plug flow.

Furthermore, it also assumed that the bed temperature is uniform, that no reaction takes place in the free board space of the fluidized bed, and that when the biomass particle enters the bed area it decomposes forming char, gas and tar.

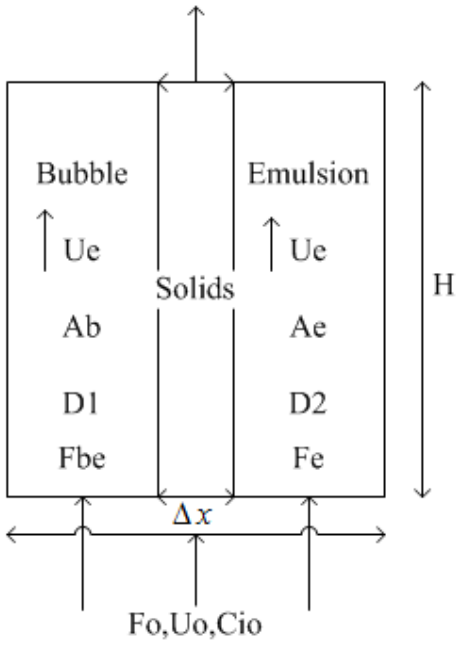

Figure 15. Derivation of Fluid Dynamic model [94]

5.1.1. Derivation of Fluid-dynamic Model Equation

In order to derive the model equation in the fluidized bed reactor, first of all, let us consider an elemental volume which is $A_b \Delta x$ in the bubble phase of the reactor, and derive a mass balance equation for a species i over the height H :

$$i_{tot} = (rate\, i_{in}) - (rate\, i_{out}) - (rate\, i_{emulsion\ \ phase}) + (rate\, i_{chemical\ reaction}) \qquad (52)$$

This can be expressed in the form

$$\frac{\partial}{\partial t}(A_b \Delta x C_{ib}) = U_b A_b C_{ib}\big|_x - U_b A_b C_{ib}\big|_{x+\Delta x} - A_b \Delta x F_{be}(C_{ib} - C_{ie}) + R_{ib} A_b \Delta x \quad (53)$$

When the reaction reaches steady state, it becomes

$$U_b \frac{dC_{ib}}{dx} = D_1 \frac{d^2 C_{ib}}{dx^2} - F_{be}(C_{ib} - C_{ie}) + R_{ib} \tag{54}$$

Similarly, for an elemental volume $A_b \Delta x$ in the emulsion phase, the equation is

$$\frac{U_e dC_{ie}}{E_{mf} dx} = D_2 \frac{d^2 C_{ie}}{dx^2} + \frac{F_{be}}{E_{mf}} * \frac{A_b}{A_e}\left(C_{ib} - C_{ie}\right) + R_{ie} \tag{55}$$

For the solid phase, the equation can be expressed in the form

$$W_{out} = W_{in} + R_{6e} \tag{56}$$

Therefore, when the reaction reaches a steady state, the boundary condition equation is as follows

When $x = 0$

$$C_{ib} - \frac{D_1 dC_{ib}}{U_b dx} = C_{i0}, i = CO, CO_2, H_2, H_2O, CH_4, Char \tag{57}$$

$$Cie - \frac{D_2 dC_{ie}}{U_e dx} = C_{i0} \tag{58}$$

When $x = H$, then $\frac{dC_{ib}}{dx} and \frac{dC_{ie}}{dx} = 0,$
$i = CO, CO_2, H_2, H_2O, CH_4, char$ (59)

Consequently, for the solid phase, when $x = H$, the function is obtained

$$\frac{dC_{sj}}{dx} = 0 \tag{60}$$

In order to calculate the hydrodynamics, three steps need to be taken into consideration, the diameter of the bubbles, the velocity of the bubbles and the volume fraction of the bubble in the fluidized bed gasifier.

Let us consider the bubble diameter equation:

$$D_b = D_{Bm}\left(D_{Bm} - D_{bo}\right) * \exp\left(-X/D\right) \tag{61}$$

The dimension of $\left(D_{Bm}\right)$ and $\left(D_{bo}\right)$ can be expressed as follows

$$D_{Bm} = \left[A * \left(U_o - U_{mf}\right)\right]^{0.4} \tag{62}$$

$$D_{bo} = \left[A * \left(U_o - U_{mf}\right)/N\right]^{0.4} \tag{63}$$

Consequently, the bubble velocity, the volume fraction of the bubble phase, the emulsion phase of the gas velocity, and finally the height of the bed can be expressed in the form.

$$U_b = U_o - U_{mf} + \left(gD_b\right)^{0,5} \tag{64}$$

$$DEL = \left(U_o - U_{mf}\right)/U_b \tag{65}$$

$$U_e = U_{mf}/\left(1 - DEL\right) \tag{66}$$

Further, the gas exchange coefficient between the bubble and emulsion phase can be expressed in the form.

$$F_{be} = X/D_b \tag{67}$$

Finally, the height of the expanded bed can be expressed in the form.

$$H = \frac{H_{mf}}{(1 - DEL)} \tag{68}$$

Where

A Cross section area, m^2

A_c Char specific surface area, m^2/m^3

C_i Mole mass of fraction i from biomass, kmol/kg of feed

C_{ib} Concentration of component i in bubble phase, $kmol/m^3$

C_{ie} Concentration of component i in emulsion phase, $kmol/m^3$

C_{io} Initial concentration of component i, $kmol/m^3$

U_b Rate of bubble, m/s

U_e Gas velocity in emulsion phase, m/s

U_{mf} Minimum fluidized velocity, m/s

W_{in} Yield of char from pyrolysis per second, kg/s

W_{out} Char outflow amount from fluidized bed, kg/s

X Axial space against the distribution board, m

C_{sj} Concentration component j in emulsion phase, $kmol/m^3$

$D_1 and\ D_2$ Reactor diameter, m

D_b Bubble diameter, m

D_{bo} Initial bubble diameter, m

D_{Bm}	Maximum bubble diameter, m
DEL	Bubble phase volume fraction, [-]
E_{mf}	Minimum fluidizing void ratio, [-]
F_{be}	Gas exchange quotient, 1/s; feeding rate= kg/s
g	9,81m/s^2
H	Height of fluidized bed, m
H_{mf}	Minimum fluidizing bed height, m
R_{ib}	Yield of component i in bubble phase per second, kmol/s
R_{ie}	Yield of component i in emulsion phase, kmol/s
R_{sj}	Yield of solid component j in emulsion phase, kg/s
k_o	Frequency factor, 1/s
k_1	Reaction rate constant of reaction j , 1/s
K_w	Equilibrium constant of water gas exchange reaction, [-]
R	Ideal gas constant, J/mol K

It could be imagined that the kinetics of the homogeneous combustion and reforming reactions are well known, but this is not the case, since the reactions between the stable chemical species involved in the homogeneous reactions are a complex combination of several elementary reactions.

Many models have been published by different authors [95], but, there is little difference between them, as all of them are based on estimation of essential elements of fluid dynamics, such as bubble velocity, bubble diameter, fraction of bubbles in the bed, velocity of gas in the emulsion, and the application of similar correlations. Table 3 presents semi empirical fluid dynamic correlations for the gas flow pattern in fluidized bed gasifiers [93].

Table 3. Semi Emperical Fluid Dynamic Correlation [93]

Name of variable	Unit	Correlation
Rising velocity of a single bubble, U_{br}	m/s	$U_{br} = 0{,}711(gd_b)^{1/2}$
Bubble velocity, U_b	m/s	$U_b = U_{br} + 1.6((U_o - U_{mf}) + 1.13 d_{b,av}^{0,5}) D_B^{1.35}$ $d_{b,av} = \frac{1}{H_x}\int_0^{H_x} d_b(h)dh$
Velocity of minimum fluidization, U_{mf} Reynolds number at minimum fluidization, $\mathrm{Re}_{p,mf}$	m/s	$U_{mf} = \mathrm{Re}_{p,mf}\left(\frac{\mu_g}{d_p \rho_g}\right)$ $\mathrm{Re}_{p,mf} = (28.7^2 + 0{,}0494 Ar)^{0,5} - 28.7 (dp > 100\mu m)$ $\mathrm{Re}_{p,mf} = (33.7^2 + 0{,}0408 Ar)^{0,5} - 33.7 (dp < 100\mu m)$ $\mathrm{Re}_{p,mf} = \sqrt{C_1^2 + C_2 Ar} - C_1 (C_1 = 27{,}2, C_2 = 0{,}0408)$
Voidage at minimum fluidization, e_{mf}		$Ar = \frac{1.75}{e^3_{mf}\phi}\mathrm{Re}^2_{p,mf} + \frac{150(1-e_{mf})}{e^2_{mf}\phi}\mathrm{Re}_{p,mf}$
Bubbles size, d_b	m	$d_b = 0{,}54(U_o - U_{mf})^{0,4}(h + 4\sqrt{A_B})^{0,8} g^{-0.2}$
Bubbles size, d_b	m	$d_b = d_{bm} - (d_{bm} - d_{bo}) e^{-0{,}3h/Dt}$ *for* $0{,}3 < Dt < 1{,}3$ $d_{bo} = 1{,}38 g^{-0{,}2}\left[A_B (U_o - U_{mf}/N_t\right]^{0,4}$ *perforated plate* $d_{bo} = 3{,}77 g^{-1}(U_o - U_{mf})^2$ *porous plate* $dbm = 2{,}5 g^{-0{,}2}\left[A_B (U_o - U_{mf}\right]^{0,4}$
Dimensionless visible velocity ψ		$\psi = 1{,}45 Ar^{-0{,}8}$ $\psi = f(h + 4\sqrt{A_o})^{0,4}$

Table 4. Semi Emperical Fluid Dynamic Correlation [93]

Dimensionless visible velocity ψ		$\psi = 1{,}45Ar^{-0{,}8}$ $\psi = f(h + 4\sqrt{A_o})^{0{,}4}$
Dimensionless visible velocity		$f_{SFB} = \left[0{,}26 + 0{,}70\exp(-33d_p)\right]\left[0{,}15 + (U_o - U_{mf})\right]^{-1/3}$ $f_{CFB} = 0{,}3121 + 0{,}129U_o^{-1} - 16{,}6dp_b - 2{,}61.10^{-5}\Delta p_{ref}$
Bubble void fraction, e_b		$e_b = \left[1 + (1{,}3/f)(U_o - U_{mf})^{0{,}8}\right]^{-1}$
Bed expansion factor, f_{bex}		$f_{bex} = 1 + \frac{(1{,}032(U - U_{mf})^{0{,}57}\rho g^{0{,}083})}{(\rho_p^{0{,}166}U_{mf}^{0{,}063}D_t^{0{,}445})}(D_t < 0{,}0635)$ $f_{bex} = 1 + \frac{14{,}31(U_o - U_{mf})^{0{,}738}d_p^{1{,}006}\rho_p^{0{,}376}}{\rho_g^{0{,}126}U_{mf}^{0{,}937}}(D_t > 0{,}0635)$
Voidage in the emulsion phase, ε_e		$\varepsilon_e = e_{mf}(U_e/U_{mf})^{1/6{,}7}$
Bubble emulsion mass transfer coefficient, K_{be}	$1/s$	$K_{be} = \frac{2U_{mf}}{db} + \frac{12(D_g e_{mf} U_b)^{1/2}}{\pi d_b^{3/2}}$
Terminal velocity U_t inside the Reynolds number at terminal velocity $\mathrm{Re}_{p,t}$	m/s	$U_t^* = \left[18/(d_p^*)^2 + (2{,}335 - 1{,}744\phi)/(d_p^*)^{0{,}5}\right]^{-1}$ $U_t^* = \mathrm{Re}_{p,t}/Ar^{1/3}; d_p^* = Ar^{1/3}; \mathrm{Re}_{p,t} = (\rho_g d_p U_t/\mu_g$

Table 5. Semi Emperical Fluid Dynamic Correction [93]

Entrainment flux of particle at the bed surface, $(h = Hx), Gx$	kg/m^2s	$G_x = 3{,}07 * 10^{-9}A_B\, d_{b,h} = H_x(\rho_g^{3{,}5}g^{0{,}5}\mu_g^{-2{,}5})(U_o - U_{mf})^{2{,}5}$
Elutriation rate constant for different particle size i entrainment flux where $dG/dh = 0; Gi,\infty = Ei,\infty$	kg/m^2s	$E\infty, i = 0{,}011\rho_p(1 - U_{t,i}/U_o)^2 \; for\, U_{t,i} < U_o$ $E\infty, i = 0\,(for\, \mathrm{U}_{t,i} > U_o)$
Decay coefficients, a and K	m^{-1}	$a = 4U_t/U$ $K = 0{,}23/(U_o - U_t)$

5.2. Aspen Plus Modeling

Different stages are considered in the Aspen Plus simulation this was done in order to show the overall gasification process for decomposition of the feed, such as volatile reactions, char gasification and gas- solid separation. For evaluation of the process flow diagram an Aspen Plus model is implemented to determine energy and material balances of the process.

5.2.1. Energy and Material Balance

Each unit operation model in Aspen Plus presents results in the form of a balance sheet that displays a summary of material and energy balance around the unit operation block. These balances represent the total of all inlet and outlet material and energy around the block.

However, steady state reactions are considered to calculate the heat of combustion and material energy balance around unit operation blocks. Consequently, the heat of combustion of wood in the HCOALGEN model is a gross calorific value. It is expressed in Btu/Ib of wood on a dry basis, and the products are in the form of ash, liquid water and gaseous products. The net calorific value can be calculated from the gross calorific value by making a deduction for the latent heat of vaporization of water [96].

As a result, Aspen Plus uses the following equations to calculate the heat of combustion and material energy balance.

Let us consider the enthalpy calculation in the form

$$\begin{aligned} fH(T) &= \sum f_i \left[H_{f,i}(T_{ref}) + \int_{T_{ref}}^{T} C_{p,i} dT \right] + f\Delta H(T \\ &= \sum f_i \left[H_{f,i}(T_{ref}) + f_i H_i(T) \right] + f\Delta H(T) \end{aligned} \tag{69}$$

Then, let us formulate the heat of combustion

$$C_\alpha H_\beta O_\gamma N_\delta S_\varepsilon + \left(\alpha + \frac{\beta}{4} + \varepsilon - \frac{\gamma}{2} \right) \rightarrow \alpha CO_{2(g)} + \frac{\beta}{2} H_2 O_{(g\ or\ l)} + \frac{\delta}{2} N_{2(g)} + \varepsilon SO_{2(g)}$$

Consequently, the lower heating value (LHV) minus water in the gas state can be calculated as follows.

$$H_{LHV, C_\alpha H_\beta O_\gamma S_\varepsilon} = -H_{f, C_\alpha H_\beta O_\gamma N_\delta S_\varepsilon} + \alpha H_{f, CO_2} + \frac{\beta}{2} H_{f, H_2O} + \varepsilon H_{f, SO_2} \tag{71}$$

Where

$(\alpha, \beta, \gamma, \delta, \varepsilon)$ Non-dimensional

Similarly, the higher heating value (HHV) minus water in the liquid state, can be calculated in the form.

$$H_{HHV, C_\alpha H_\beta O_\gamma N_\delta S_\varepsilon} = H_{LHV, C_\alpha H_\beta O_\gamma N_\delta S_\varepsilon} + \frac{\beta}{2} \Delta H^{vap}_{H_2O}(T_{ref}) \tag{72}$$

The gas efficiency through this combustion process needs to be calculated. But first the ratio of the higher heating value of the biofuel produced and the higher heating value of the wood needs to be calculated.

$$Gas\ Efficiency = \frac{HHV_{fuel} * \eta_{fuel}}{HHV_{wood} * M_{wood}} \tag{73}$$

$$HHVfuel = \left(A'*y_{H2} + B*y_{CO} + C*y_{CH_4} + D*y_{H_2O}\right) \tag{74}$$

The molar flow rate of $\left(y_{H_2}\right), \left(y_{CO}\right), \left(y_{CH_4}\right)$ $\left(y_{H_2O}\right)$ and $\left(Q\right)$ can be calculated according to the following equations

$$n_{H2} = \frac{\left(1 - wt\%_{moisture}\right) * \left(wt\%_{hydrogen} * m_{wood}\right)}{M_{H_2}} \tag{75}$$

$$n_{CO} = \frac{\left(1 - wt\%_{moisture}\right) * \left(wt\%_{CO} * m_{wood}\right)}{M_{CO}} \tag{76}$$

$$n_{CH_4} = \frac{\left(1 - wt\%_{moisture}\right) * \left(wt\%_{CH_4} * m_{wood}\right)}{M_{CH_4}} \tag{77}$$

$$n_{H_2O} = \frac{\left(wt\%_{moisture}\right) * m_{wood}}{M_{H_2O}} \tag{78}$$

$$Q = m_{wood} * Cp\Delta T \tag{79}$$

Additionally, the mass flow rate of the ash is calculated according to the Equation 80

$$m_{ash} = (1 - wt\%_{moisture}) * (wt\%_{ash} * m_{wood}) \tag{80}$$

Let us consider the heat of combustion related to the heat of formation in the form.

$$\begin{aligned} &\sum_i (F_{i,in} - F_{i,out}) H_{f,i} = \sum_i (F_{i,in} - F_{i,out})(-H_{c,i}) + \left[\sum_i (F_{ci,in} - F_{ci,out})\right] H_{f,CO_2} \\ &+ \left[\sum_i (F_{H,in} - F_{H,out})\right] H_{f,H_2O} + \left[\sum_i (F_{s,in} - F_{s,out})\right] H_{f,SO_2} \end{aligned} \tag{81}$$

Let us assume that

$$\left[\sum_i (F_{ci,in} - F_{ci,out})\right], \left[\sum_i (F_{H,in} - F_{H,out})\right] \text{and} \left[\sum_i (F_{s,in} - F_{s,out})\right] = \text{O} \tag{82}$$

Therefore, the heat of formation can be written as follows.

$$\sum_i (F_{i,in} - F_{i,out}) H_{f,i} = \sum_i (F_{i,in} - F_{i,out})(-H_{c,i}) \tag{83}$$

Furthermore, let us consider energy and material balances as shown in Figure 16.

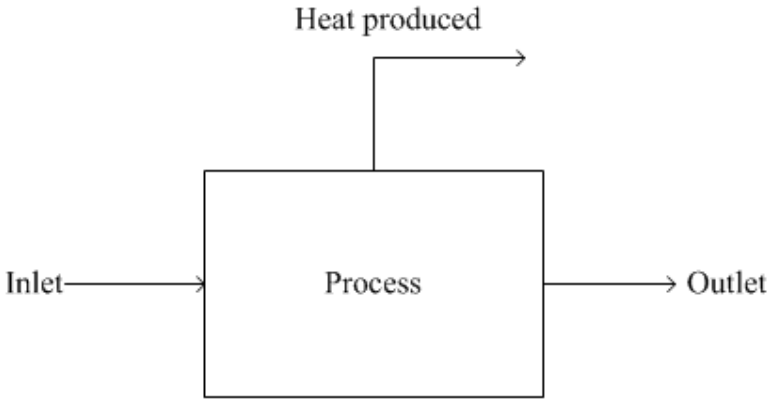

Figure 16 . Energy and material balance

$$\begin{aligned} 0 &= Energy\ in - Energy\ out \\ 0 &= F_{i,in}\, H_{f,i}(T_{in}) - F_{i,out}\, H_i(T_{out}) - Q \end{aligned} \tag{84}$$

The dimension Q can be defined as follows

$$\begin{aligned} Q = &\sum_i \left(F_{i,in} - F_{i,out}\right)\left(H_{f,out}\right)\left(T_{ref}\right) + \sum_i \left[F_{i,in} H_{i,in}(T_{in}) - F_{i,out} H_{i,in}(T_{out})\right] \\ &+ \left[F_{i,in}\Delta H(T_{in}) - F_{i,out}\Delta H(T_{out})\right] \end{aligned} \tag{85}$$

Where

HHV_{fuel}	Higher heating value of fuel, MJ/kg
HHV_{wood}	Higher heating value of wood, MJ/kg
n_{fuel}	Molar flow rate of fuel gas, [-]
n_{wood}	Mass flow rate of wood, kg/hr
y_{H_2}	Mole fraction of H_2 in the fuel gas [-]
y_{CO}	Mole fraction of CO in the fuel gas [-]

y_{CH_4}	Mole fraction of CH_4 in the fuel gas [-]
Q	Heat duty, kJ/hr
m_{wood}	Mass flow rate of the wood, kg/hr
Cp	Specific heat capacity of gases, J/kmol.K
ΔT	Temperature difference, K
m_{ash}	Mass flow rate of the ash, kg/hr
M	Molecular weight, g/mole
$F_{i,in}$	Molar flow rate of the feed, kmol/hr
$H_{i,in}$	Molar enthalpy of the feed, kJ/mole
$F_{i,out}$	Molar flow rate of product, kmol/hr
$H_{f,out}$	Molar enthalpy of product, kJ/mole

5.3. Process Design Specifications

A design specification sets the value of a variable that Aspen Plus calculates, for example, product stream purity or the maximum permissible amount of an impurity in a recycle stream may be desired. For each design specification, a block input variable, process feed stream variable, or other simulation input might be identified and manipulated to meet the standard specified. For example, a purge flow rate might be manipulated to control the level of impurities in a recycle stream. In general, the design specification can be used to simulate the steady state effect of a feedback controller.

Throughout this work, design specifications calculate the inlet and outlet enthalpy of the selected blocks For instance, the temperature of the block “heat exchanger” is chosen as a manipulated variable. Therefore, the inlet and outlet enthalpies, and the inlet temperature of the block heat exchanger are set. However, they are all stream variables. To sum up, convergence of the design specification does not have to be specified; Aspen Plus will automatically generate a convergence block to converge the specification.

5.4. Components Model and Equipment Specifications

The Aspen Plus simulation model simulates integrated wood biomass gasification with a Fischer Tropsch synthetic reactor. The Aspen Plus simulation model includes the components, unit operation, and equipment specifications given in Table 6 and Table 7.

Table 6. Component Model

Component ID	Types	Component Name	Formula
Wood	Nonconventional	-	-
Ash	Nonconventional	-	-
C	Conventional	Carbon graphic	C
O_2	Conventional	Oxygen	O_2
N_2	Conventional	Nitrogen	N_2
H_2O	Conventional	Water	H_2O
Cl_2	Conventional	Chlorine	Cl_2
S	Conventional	Sulfur	S
CO	Conventional	Carbon monoxide	CO
CO_2	Conventional	Carbon dioxide	CO_2
NO	Conventional	Nitric oxide	NO
NO_2	Conventional	Nitrogen dioxide	NO_2
CH4	Conventional	Methane	CH_4
H2	Conventional	Hydrogen	H_2
C_2H_4	Conventional	Ethylene	C_2H_4
C_2H_6	Conventional	Ethane	C_2H_6
C_3H_8	Conventional	Propane	C_3H_8
C_4H_{8-1}	Conventional	1-Butene	C_4H_{8-1}
C_5H_{12-1}	Conventional	N-Pentane	C_5H_{12-1}
C_6H_6	Conventional	Benzene	C_6H_6
C_7H_8	Conventional	Toluene	C_7H_8
C_8H_{18-1}	Conventional	N-Octane	C_8H_{18-1}
$C_{10}H_8$	Conventional	Naphthalene	$C_{10}H_8$
$C_{12}H_{26}$	Conventional	N-Dedecane	$C_{12}H_{26}$
$C_{17}H_{36}$	Conventional	N-Heptadecane	$C_{17}H_{36}$

Table 7. Equipment Specifications

Unit Operation	Aspen Plus Model	Equipment Specifications
Wood Sizing	Crusher, Screen	Reduce wood particle size
Decomposer	RYield	Wood composed to produce yield gas component
Wood Gasification	RGibbs	Decompose wood to produce gas
Cyclone	Ssplit	Separate solid (Ash and Char)
Gas Scrubber	Flash2	Removal of acid gases and Tars
WGS	REquil	Convert CO to CO2
Cooling	Heater	Convert higher to lower temperature
Fischer Tropsch	RCSTR	Predict gas flow rate and stream enthalpy
Gas Separation	Flash3	Separate FT off-gases and liquid gas
Heat Exchanger	Heater	Increase temperature
Gas Compressure	Compressor	Calculate power required
Gas Burner	RGibbs	Natural Gas completed burn with temperature and pressure
Gas Turbine	Compressor	Calculate power required
Refining	Radfrac	Split fraction product stream for gasoline and diesel

5.4.1. Aspen Plus Simulation Results

The material and energy balance of the process was modeled using Aspen Plus, the only commercially available software capable of handling wood and solid components.

5.4.1.1. Simulating the Wood Feed Stream

Although, Aspen Plus has a component named wood in its solid databank, it is not the component used in the simulation. Instead, wood was simulated as a nonconventional solid, as suggested by an Aspen Plus tutorial on simulation of coal combustion. However, when simulating wood as a nonconventional solid, the following fields must be taken into account; proximate analysis, ultimate analysis and heating value. Table 6 above presents a list of the nonconventional properties entered for the wood stream.

5.4.1.2. Simulating the Wood Gasifier

As Figure 17 shows, the wood gasifier is simulated in two different blocks, DECOMP and GASIFIER. The first block, DECOMP, is simulated as a Yield Reactor. The input to this block is the wood stream as simulated above. For this specific process, the products of the reaction are the wood constituents in element form, where carbon, nitrogen, oxygen, hydrogen, sulfur, water and ASH become just ASH.

The product yields of this reaction are calculated from the proximate and ultimate analysis, and these results are used to specify the yields for the Aspen yield reactor. The second reactor, GASIFIER, is simulated as a Gibbs Reactor. A Gibbs reactor is used to model reactions that come to equilibrium by calculating the chemical and phase equilibriums from minimization of the total Gibbs free energy of the system. The inputs to this block are the decomposed wood stream, pressurized oxygen, and the energy from the DECOMP reactor.

The following product reactions are treated; methane, hydrogen, carbon monoxide, carbon dioxide, water, ammonia, hydrogen sulfide, nitrogen, tars, and unreacted CHAR and ASH. In reality, the reactors DECOMP; GASIFIER and CYCLONE represent a single gasifier; a circulating fluidized bed gasifier.

In addition to simulating the feed components and products, certain reaction conditions must be specified: pressure, temperature and heat duty and feed conditions. The gasifier is simulated as an adiabatic process, and the temperature is maintained by creating a design specification that adjusts the amount of process water used in the wood drying. The process water is available at 1000 ^{o}C.

The gasifier pressure is the pressure used for the entire process, which is 1 bar, based on the gasification process, and air is available at 1 bar and 130 ^{o}C. However, compressor air is necessary to compress air to the gasifier pressure of 1 bar and a pump is also necessary to raise the pressure of the water in the DECOMP reactor. Figure 17 presents an overview of the Aspen Plus Simulation process and Table 6 present Aspen Plus Simulation results.

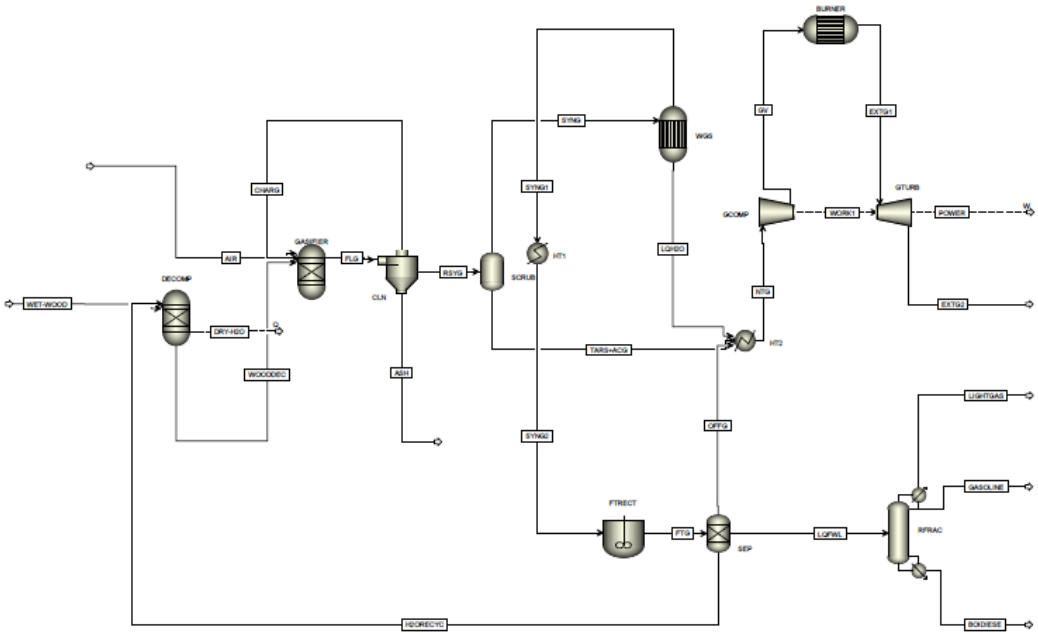

Figure 17. Aspen plus Simulation process overview

Table 8. Aspen Plus Simulation Table Results

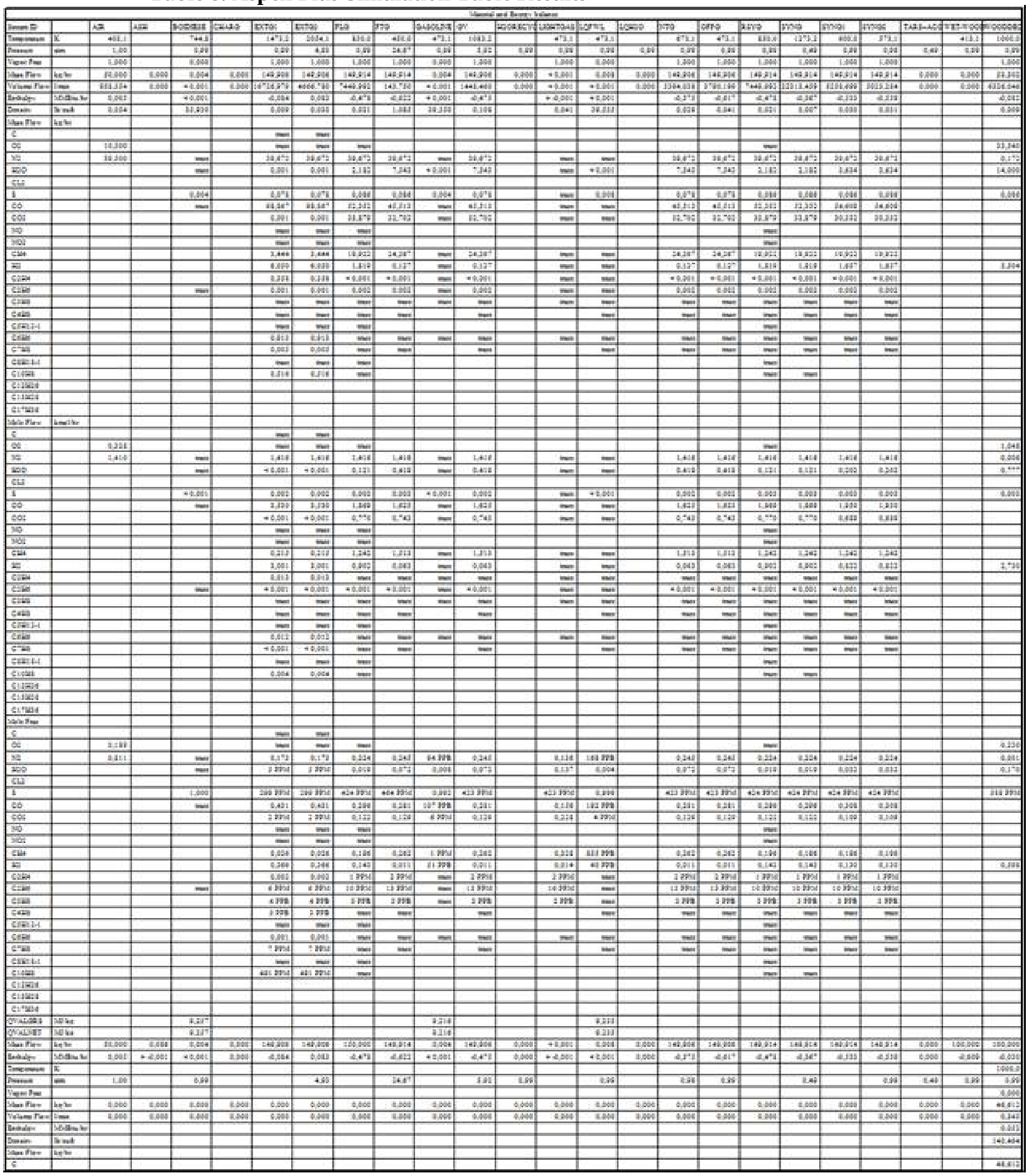

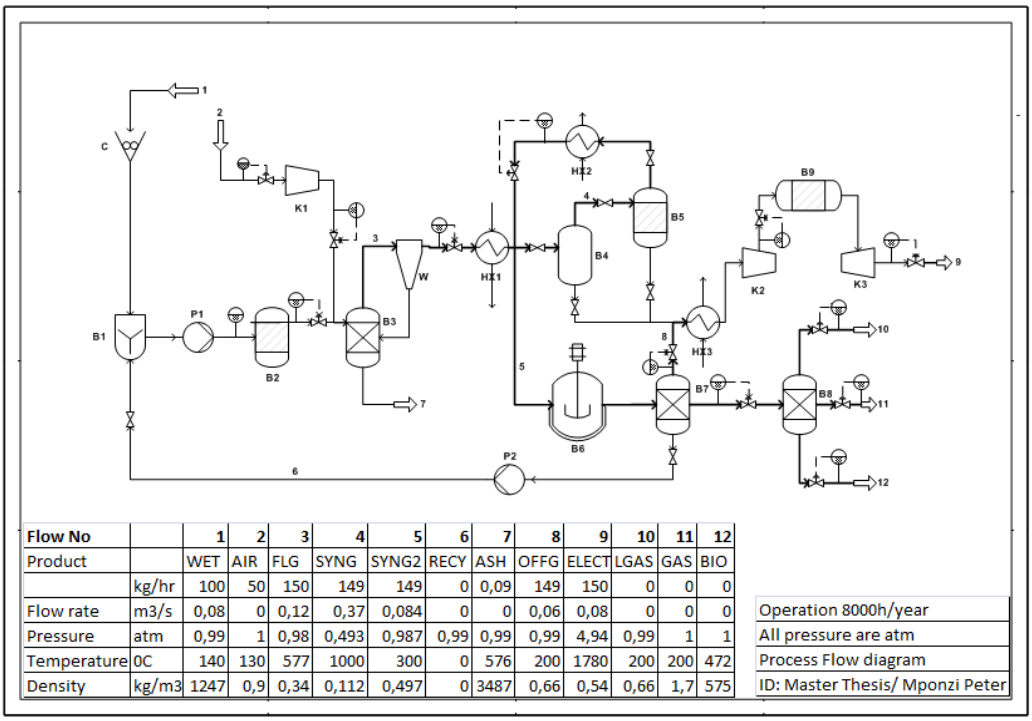

Flow No		1	2	3	4	5	6	7	8	9	10	11	12
Product		WET	AIR	FLG	SYNG	SYNG2	RECY	ASH	OFFG	ELECT	LGAS	GAS	BIO
	kg/hr	100	50	150	149	149	0	0,09	149	150	0	0	0
Flow rate	m3/s	0,08	0	0,12	0,37	0,084	0	0	0,06	0,08	0	0	0
Pressure	atm	0,99	1	0,98	0,493	0,987	0,99	0,99	0,99	4,94	0,99	1	1
Temperature	0C	140	130	577	1000	300	0	576	200	1780	200	200	472
Density	kg/m3	1247	0,9	0,34	0,112	0,497	0	3487	0,66	0,54	0,66	1,7	575

Operation 8000h/year
All pressure are atm
Process Flow diagram
ID: Master Thesis/ Mponzi Peter

Figure 18. Economic Analysis of Biomass Gasification via Fischer Tropsch synthesis

5.4.1.3. Sensitivity Analysis

In the Aspen Plus simulation, sensitivity analysis was used to observe the effect of temperature on the GASIFIER reactor, WGS reactor and FT Synthetic reactor.

5.4.1.3.1. Effect of Temperature on Gasifier

A gasification temperature of 700^{o}C and 850^{o}C was used to simulate the effect of temperature on the gasifier in the circulating fluidized bed. The lower gasifier temperature, the better results for the yield gas components. At lower gasification temperature, more water is required in the biomass to maintain the reactor temperature.

Since water reacts with biomass, less oxygen is required to drive the gasification reaction. Consequently, higher cold gas efficiency is achieved at lower temperatures. This could imply that gasification with water yields, more combustible products than with oxygen.

As a result, lowering the reactor temperature from 1000 ^{o}C -850 ^{o}C and raising the water gas shift temperature from 400 ^{o}C – 600 ^{o}C can improve overall gas efficiency, and power production. Similarly, The Fischer Tropsch offgas is converted into a gas turbine and finally biodiesel is produced as a fuel for transportation. Figure 19 presents the effects of temperature on the gasifier.

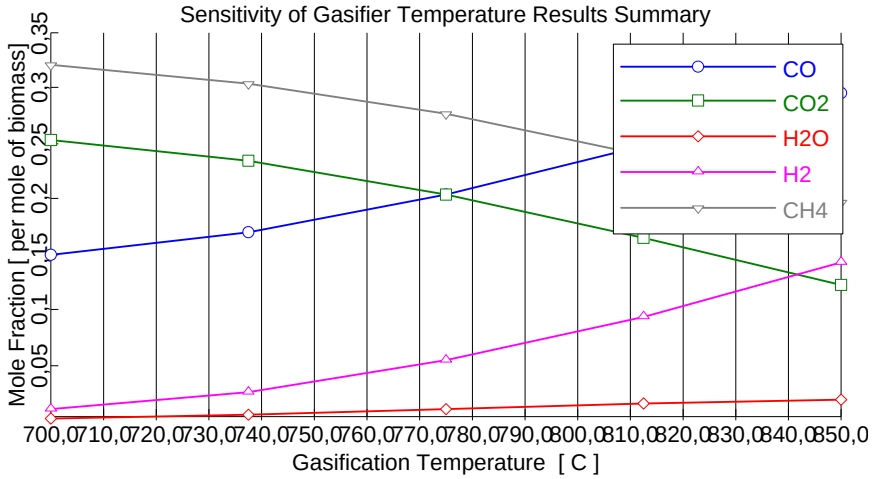

Figure 19. Effect of temperature on gasifier

5.4.1.3.2. Effect of Temperature on Heating Value

The effect of gasification temperature on the heating value will depend on the composition of the gases during combustion or gasification. As shown in Figure 20. The heating value of the flue gas increases with increasing temperature

Therefore, gasifier temperature should be sufficiently high to produce non condensable tars in order to avoid problems in downstream conversion. Moreover, condensable tars must be avoided when the product gas is used in an engine or gas turbine.

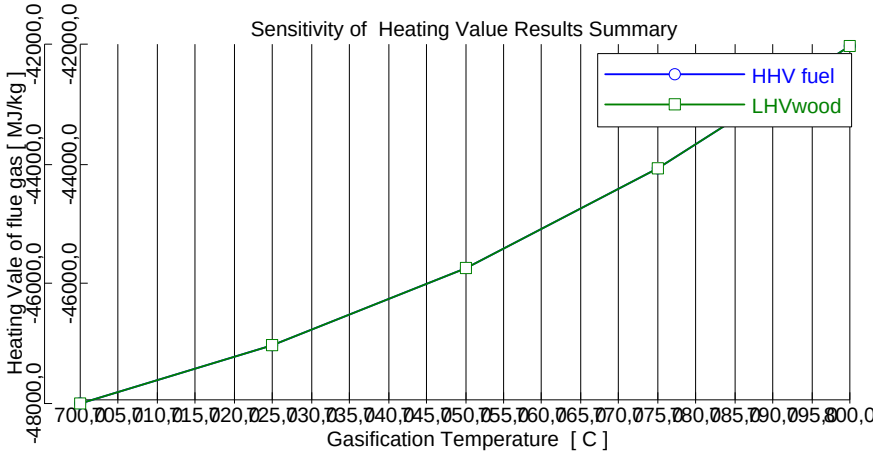

Figure 20. Effect of temperature on heating value of syngas

5.4.1.3.3. Effect of Temperature on Water Gas Shift Reactor

In commercial gasifiers, the produced syngas contains high amounts of carbon monoxide, about 30-60% [97] of which can be converted to hydrogen by water gas shift reaction. Un-shifted syngas contains 27-50% of carbon monoxide [78].

If the shift reaction is carried out after removal of sulfur from the syngas, it is called a sweet-gas shift reaction; if it is done before sulfur removal, then it is called a sour-gas shift reaction. A sweet-gas shift reaction comprises high temperature and low temperature reactions; the conversion stages are taken between the reactors

The temperature used in the water gas shift was 500 ^{o}C – 600 ^{o}C. Raising the water gas shift reaction temperature can improves gas efficiency, which in turn leads to better production of ultra clean syngas for the Fischer Tropsch synthetic reactor.

Consequently, gas efficiency is improved because less oxygen is required in the gasifier feed to satisfy the design constraints. Figure 21 presents the effect of temperature on water gas shift reactor.

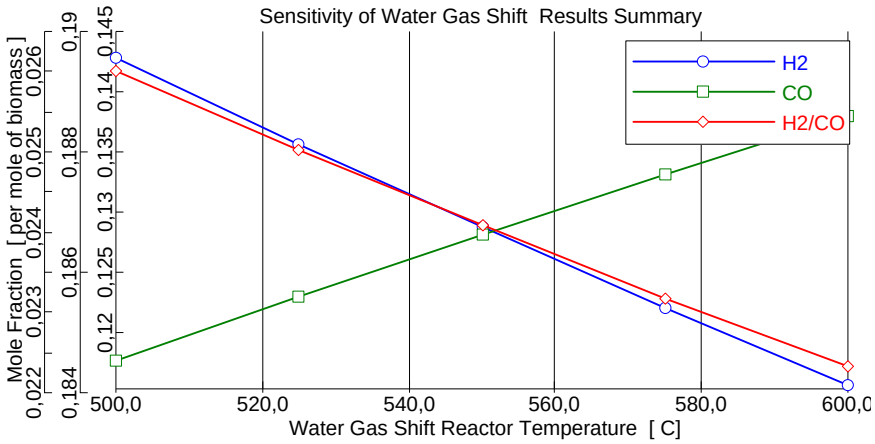

Figure 21. Effect of temperature on water gas shift reactor

5.4.1.3.4. Effect of Temperature on Fischer Tropsch Reactor

The effect of temperature on the Fischer Tropsch reactor is shown in Figure 22. Low mole flow rates of steam produced gas with a low H2/CO ratio suitable for the Fischer Tropsch synthesis, while higher mole flow rates of steam produced gases such as carbon monoxide, carbon dioxide, hydrogen and methane.

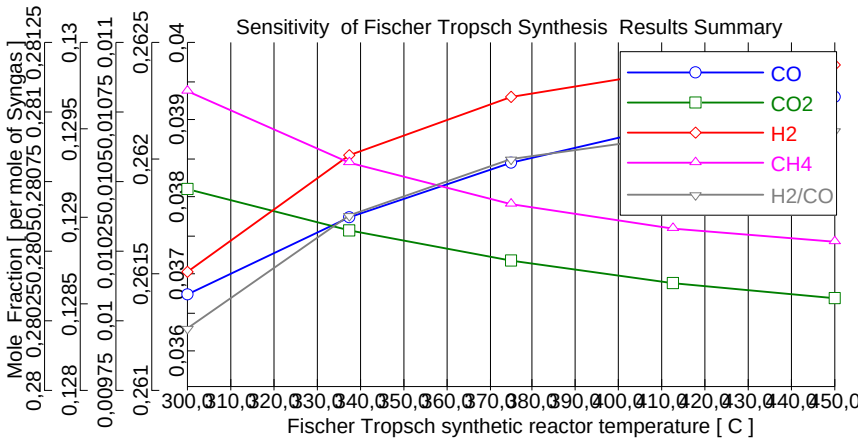

Figure 22. Effect of temperature on Fischer Tropsch synthetic reactor

6. ECONOMIC ANALYSIS

This economic analysis is presented in Figure 18 process flow diagram shows combination of the biomass gasification via by Fischer Tropsch synthesis. Due to the lack of an industrial database, different costs are estimated and calculated based on cost data available from the website www.matche.com. Despite this limitation, the economic analysis will give an idea about the cost and profitability of the entire system presented.

6.1. Cost Estimation

Once the final design stage is completed, it becomes possible to make cost estimations because detailed information is available for the equipment specifications, as given in Table 9.

Table 9. Total Equipment Items Costs

EQUIPMENTS	EUROS: €
Drying Reactor	140000
CFB gasifier	570000
Cyclone	30000
Cooler	70000
Gas Scrubber	60000
WGS Reactor	70000
Heat exchanger	30000
Fischer Tropsch Reactor	90000
Flash3 Separation Reactor	20000
Gas Compressor	50000
Burner Reactor	80000
Gas Turbine	50000
Radfrac Separation Reactor	10000
Total purchase Equipment items Costs	**1270000**

6.1.1. Investment Costs

The total investment costs for the plant are not just costs for the main plant items but also for installation, engineering and contractors. However, other costs also need to be taken into account, for example, total equipment items costs. Consequently, a total investment cost can be obtained by adding 5% working capital of fixed capital costs. Using the costs given above, the total investment cost is estimated to be 4.9 million Euros. Table 10 presents total investment costs.

Table 10. Total Investment Costs

ITERMS PROCESS EQUIPMENT COSTS	**SOLID PROCESS FACTORS**
1.Major Equipment Costs	Stainless steel
Equipment (f1)	0,15
Piping(f2)	0,25
Instrumentation (f3)	0,12
Electrical(f4)	0,2
Building process(f5)	0,05
Site development(f6)	0,05
Auxillary Facilities (f7)	0,3
∑(factor)	1,12
2.Total physical plant costs (PPC)	Euros: €
PPC= PCE*∑(factor) (1+f1+f2+f3+f4+f5+f6+f7)	**3020000**
Design & Engineering (f10)	0,33
Contractors's fee (f11)	0,17
Contingency (f12)	0,34
∑(factor)	0,84
Fixed Capital= PPC*∑(factor) (1+f10+f11+f12)	**4670000**
Working Capital +- 5% of Fixed Capital Costs	230000
Total Investment Costs	**4900000**

6.1.2. Operation Costs

The operation costs are divided into two main parts; fixed operation costs, and variable operation costs. This work focuses on total investment costs, fixed operation costs, and variable operation costs. Table 11 presents total operating costs.

Table 11. Total Operating Costs

	Euros: €
Total fixed operating costs	704000
Total variable operating cost	7000
Total operation costs	**711000**

6.1.3. Fixed Operation Costs

The main parts to be considered when calculating fixed operation costs are; Operating labor, supervision, plant overheads, maintenance. In the calculations, operating labor work is calculated at ca. 40h/week and the salary for a worker is considered approximately 4000 €/month. Table 12 presents total fixed operation costs.

Table 12. Fixed Operation Costs

	Percent :%	Euros : €
Work Salary per month		4000
Operating labor Costs		320000
Supervision Cost, +-35% OpLabCost	0,35	110000
Maintenance Costs, +-4 % FCI	0,04	190000
Plant Overhead Cost ,+-3% FCI +70% OpLabCost	0,03	80000
Total Fixed Operation Costs		**704000**

6.1.4. Variable Operation Costs

Variable operating costs are costs dependent on the production rate. Variable operating costs are based on the utilities and raw materials needed for operations in the plant.
In this design, the utilities and raw materials which are taken into account are wood, as the raw material, electricity, steam and water and natural gas for start up. Annual working time is approximated to be 8000hrs in the production rate, mass flow rate and enthalpies of utilities are taken into account in the calculations.

The total amount of energy produced is approximately 130MWh for the entire systems. The price of electricity is 77€ kWh obtained from Aspen Plus simulation results. The total amount of flow rate into the gasifier including steam/air and wood as raw material is ca. 150kg/hr (0.042kg/s).

The price of steam or air is 20€ kWh. The price of forest residues as a wood raw material is 10€/t presented by E. Vakkilainen, Pöyry industry Oy, personal communication, 2007. The price of water used in the RYield reactor for drying purposes is 0.80€ /m^3. The price of natural gas for starting up reactor is approximately 0.17€/t presented by E. Vakkilainen, Pöyry industry Oy, personal communications, 2007.

The price of FT liquids is 650€/t presented by E. Vakkilainen, Pöyry industry Oy, personal communications, 2007. The total variable operation cost is approximately 7000.00€ Table 13 presents the variable operation costs.

Table 13. Variable Operation Costs

Utilities	**Euros: €**
Electricity (77€/KWh)	700
Steam/Air (20€/KWh)	200
water (0,80€/m3)	10
FT liquids selling price(650€/t)	6000
Wood purchase pricel (10€/t)	100
Natural gas purchase price	2
Total variable operation costs	**7000**

6.2. Profitability

The main purpose of investment is to make a profit. In this feasibility study, two main key figures were calculated to describe the profitability: the internal rate of return (IRR) and payback period of the investment. Table 14 presents the results of the profitability calculations. The lifetime of the investment was 6 years, so the internal rate of return was calculated based on the lifetime of investment. The working capital and fixed operating cost were estimated based on the literature [98] Taxes, insurance and depreciations are not included in the profitability calculation of this feasibility study.

Table 14. Cost data for Feasibility Calculations

	Costs	Units
Electricity selling/ purchase prise	77	€/KWh
Steam/Air purchase price	20	€/KWh
Water purpase price	0,8	€/m3
FT liquids selling price,	650	€/t
Wood purchase price	10	€/t
Natural gas purchase price	0,17	€/t

6.2.1. Internal Rate of Return

The internal rate of return is a method used for comparing the profitability of different investment. Mathematically, it is defined as the discount rate that makes the net present value of the investment equal to zero.

A project can have a good investment if its internal rate of return is greater than the rate of return that could be earned by alternative investments. The internal rate of return can be calculated as follow, and Table 15 presents investment of internal rate of return.

$$NPV = 0 = Initial\ investment + \sum_{t=1}^{N} \frac{C_F}{(1+IRR)^t} \quad (86)$$

Where

NPV	Net present value
IRR	Internal rate of return
C_F	Cash flow
t	Lifetime of the investment

Table 15. Investment of Internal Rate of Return

Column A	Column B
Description	Euros: €
Total Investment Costs	-4900000
Annual Capital Costs	7690000
Internal rate of return	3 %

6.2.2. Payback Period

Payback period is the time required after the start of the project to pay off the initial investment from the income. The payback period can be calculated as follow, and Table 16 presents investment back pack in a one year.

$$Payback\ period = \frac{Initial\ Investment\ Costs}{Cash\ Flow} \tag{87}$$

Table 16. Payback Period of Investment

	Euros: €
Initial Investment Costs	4900000
Annual Cost flow	6979000
Payback period (in year)	1

7. SUMMARY AND DISCUSSION

Production of biofuel via biomass gasification followed by Fischer Tropsch synthesis is of considerable interest because of the high quality of fuels produced, which do not contain sulphur and are free of carbon dioxide.

Aspen Plus simulation was carried out for integrated woody biomass gasification together with Fischer Tropsch synthesis. The simulation results were used to size process equipment and carry out an economic evaluation. The parameters were modeled base on the gasifier conditions, such as temperature and pressure, and also water gas shift steam ratio and Fischer Tropsch synthesis.

The most problematic and difficult part for production of biofuels is the gas cleaning process. Biomass contains a lot of tars forming compounds, so the tar content of the gasification gas might cause problems. Another difficultly is that the main of the processes operate at high temperature and pressure, whereas most conventional gas cleaning methods use low temperature and pressure. However, in this Master's Thesis used low temperature and pressure, therefore was no a need to have extra heat exchanger in the process.

An economic evaluation was carried out for each piece of equipment used. The results show that lowering the reactor temperature from 1000 ^{o}C -850 ^{o}C and raising the water gas shift temperature from 500 ^{o}C – 600 ^{o}C can improve overall gas efficiency, which in turn leads to better production of ultra clean syngas for the Fischer Tropsch synthetic reactor. Similarly, the Fischer Tropsch offgas is converted into a gas turbine for power production, and finally biodiesel is produced as a fuel for transportation.

The investment costs have not been calculated in very sufficiently details, because of the missing the industrial database. The mass and energy balances of integrated systems using Aspen Plus simulation still need to be examined to see whether the extra energy can be utilized, and the most importantly is the technologies for gas cleaning still need to be developed to the high level that enable utilize biomass gasification.

The calculation part of this Master's Thesis attempts to be examine some of the uncertainties mentioned above in further detail and determine if the process has penitential to be studied further.

8. CONCLUSIONS

Biomass gasification integrated with a Fischer Tropsch synthesis offer clear benefits for production of biofuels, as a fuel for transportation. The investment cost is significant lower. According to the profitability calculations, the internal rate of return is 3%, with payback period of 1 year. The profitability depends on the production rate, the price of raw materials, electricity and products.

The production of biofuels is determined by the availability of low cost forest residues as a raw material It is clear that a larger biofuels production rate gives better internal rate of return and shorter payback period as the results shown that the production rate is 130MWh. It also seems to be clear that it is more profitable to use the woody biomass for production of biofuels than for heat and power production.

My conclusion is that, if there are enough forest residues available for a biofuels production about 600MWh or more, it is advisable to invest in biofuels production instead of the power boiler.

9. RECOMMENDATION

The main goal and purpose for feasibility study of biomass gasification integrated with Fischer Tropsch synthesis was to design a simple model for production of biofuels and calculating the material and energy balances using Aspen Plus. Calculation was done for each piece of equipment used. It is important to find out if it more profitable to use biomass both for electricity and biofuel production In additional to the material and energy balance calculations, also an investment costs for production of biofuel was calculated. The cost was then used to calculate the profitability of the feasibility study.

Due to the critical values, such as the investment costs, the price of the raw material and the selling price of the product are still very uncertain. Costs analysis was one the most important part of this feasibility study. It is crucial to know how easily the profitability of the possible investment is affected by variations in the main key factors.

Additional to financial support through taxation, an increase the price of natural gas, or penalties for carbon dioxide emissions would make this process more economically feasible In addition to economic considerations, technical issues must also be taken into account Since all material and energy balance in the simulation were based on thermodynamic equilibrium, kinetic limitations should be investigated further.

Moreover, the gas cleaning process through the water gas shift reactor should be investigated further, running the Fischer Tropsch synthetic reactor at higher temperature would require less hydrogen and carbon monoxide to be separated from the water gas shift product.

REFERENCES

[1] A. A. Lappas, S. Bezergianni and I. A. Vasalos, "Production of biofuels via co-processing in conventional refining processes," *Catalysis Today,* vol. 145, pp. 55-62, 7/15. 2009.

[2] H. Boerrigter, H. P. Calis, D. J. Slort and H. Bodenstaff, "Gas cleaning for integrated biomass gasification (BG) and Fischer-Tropsch (FT) systems; experimental demonstration of two BG-FT systems," *Acknowledgement/Preface,* pp. 51, 2004.

[3] S. Teir., *Steam Boiler Technology.* Espoo: Helsinki University of Technology, 2003,

[4] P. McKeough., *Process Evaluations and Design Studies in the UCG Project 2004-2007 /.* VTT,: Espoo :, 2008,

[5] C. N. Hamelinck, A. P. C. Faaij, H. den Uil and H. Boerrigter, "Production of FT transportation fuels from biomass; technical options, process analysis and optimization, and development potential," *Energy,* vol. 29, pp. 1743-1771, 9. 2004.

[6] R. Krishna and S. T. Sie, "Design and scale-up of the Fischer–Tropsch bubble column slurry reactor," *Fuel Process Technol,* vol. 64, pp. 73-105, 5. 2000.

[7] I. Hannula and E. Kurkela., "A semi-empirical model for pressurized air-blown fluidized-bed gasification of biomass," *Bioresour. Technol.,* vol. 101, pp. 4608-4615, 6. 2010.

[8] W. Doherty., A., Reynolds and D. Kennedy., "The effect of air preheating in a biomass CFB gasifier using ASPEN Plus simulation," *Biomass Bioenergy,* vol. 33, pp. 1158-1167, 2009.

[9] C. Di Blasi., G. Signorelli., C. Di Russo and G. Rea., "Product Distribution from Pyrolysis of Wood and Agricultural Residues," *Industrial and Engineering Chemistry Research,* vol. 38, pp. 2216-2224, 1999.

[10] A. Faaij., "Bio-energy in Europe: changing technology choices," *Energy Policy,* vol. 34, pp. 322-342, 2. 2006.

[11] E. Kurkela., P. Ståhlberg., P. Simell., J. Leppälahti., "Updraft gasification of peat and biomass," *Biomass,* vol. 19, pp. 37-46, 1989.

[12] V. Belgiorno., G. De Feo., and C. Della Rocca., "Energy from gasification of solid wastes," *Waste Manage.,* vol. 23, pp. 1-15, 2003.

[13] E. Sipilä, J. Vehlow, P. Vainikka, C. Wilén and K. Sipilä, "Market potential of high efficiency CHP and waste based ethanol in European pulp and paper industry,"

[14] Zevenhoven. M., *Ash-Forming Matter in Biomass Fuels, Academic Dissertation , Åbo Akademi University, Turku, Finland (2001), ISBN 952-12-0813-9.* 2001,

[15] E. Kurkela., "Review of Finnish biomass gasification technologies, Report VTT Process, Espoo, 2002,"

[16] M. Siro, "Operation experiences from bark gasification for a lime kiln," in *Proc. Symp. on Low-Grade Fuels, Helsinki,* 1989, pp. 12-14.

[17] J. Palonen, J. Nieminen and E. Berg, "Thermie demonstrates biomass CFB gasifier at Lahti," *Modern Power Systems,* vol. 18, pp. 37-41, 1998.

[18] P. Basu.,. (2006, *Combustion and Gasification in Fluidized Beds, CRC, 498p ISBN 9780849333965, 2006.*

[19] P. N. P. Basu. , "Heat transfer to walls of a circulating fluidized-bed furnace," *Chemical Engineering Science,* vol. 51, pp. 1-26, 1. 1996.

[20] M. Koksal, M. R. Golriz and F. Hamdullahpur, "Effect of staged air on heat transfer in circulating fluidized beds," *Appl. Therm. Eng.,* vol. 28, pp. 1008-1014, 6. 2008.

[21] A. Dutta and P. Basu., "An improved cluster-renewal model for the estimation of heat transfer coefficients on the furnace walls of commercial circulating fluidized bed boilers," *Journal of Heat Transfer,* vol. 126, pp. 1040, 2004.

[22] P. Basu., *Circulating Fluidized Bed Boilers: Design and Operations.* Butterworth-Heinemann, 1991,

[23] H. S. Mickley and D. F. Fairbanks, "Mechanism of heat transfer to fluidized beds," *AICHE J.,* vol. 1, pp. 374-384, 1955.

[24] D. G. M. Syamlal. , "Hydrodynamics of fluidization: prediction of wall to bed heat transfer coefficients," *AICHE J.,* vol. 31, pp. 127-135, 1985.

[25] N. I. Gelperin and V. G. Einstein., "Heat transfer in fluidized beds," *Fluidization,* vol. 471, 1971.

[26] P. D. Noymer, "Cluster motion and particle-convective heat transfer at the wall of a circulating fluidized bed," *Int. J. Heat Mass Transfer,* vol. 41, pp. 147-158, 1998.

[27] M. C. Lints and L. R. Glicksman., "Parameters governing particle-to-wall heat transfer in a circulating fluidized bed," *Circulating Fluidized Bed Technology IV, AIChE, New York,* pp. 297–304, 1994.

[28] M. R. Golriz and B. Sundén, "An analytical-empirical model to predict heat transfer coefficients in circulating fluidized bed combustors," *Heat and Mass Transfer,* vol. 30, -05-16. 1995.

[29] Yu. S. Teplitskii and E. F. Nogotov, "Mixing of Particles in a Circulating Fluidized Bed," *Journal of Engineering Physics and Thermophysics,* vol. 75, -11-02. 2002.

[30] P. D. Noymer and L. R. Glicksman, "Descent velocities of particle clusters at the wall of a circulating fluidized bed," *Chemical Engineering Science,* vol. 55, pp. 5283-5289, 11. 2000.

[31] R. L. Wu, C. J. Lim, J. R. Grace and C. M. H. Brereton, "Instantaneous local heat transfer and hydrodynamics in a circulating fluidized bed," *Int. J. Heat Mass Transfer,* vol. 34, pp. 2019-2027, 8. 1991.

[32] P. Basu., "Heat transfer in high temperature fast fluidized beds," *Chemical Engineering Science,* vol. 45, pp. 3123-3136, 1990.

[33] R. L. Wu, J. R. Grace and C. J. Lim, "A model for heat transfer in circulating fluidized beds," *Chemical Engineering Science,* vol. 45, pp. 3389-3398, 1990.

[34] M. Brewster., "Effective absorptivity and emissivity of particulate slender with application to a fluidized beds," *Circulating Fluidized Bed Technology IV,* pp. 137-144, 1986.

[35] P. Basu., *Boilers and Burners : Design and Theory.* New York: Springer, 2000,

[36] S. Syahrul, I. Dincer and F. Hamdullahpur, "Thermodynamic modeling of fluidized bed drying of moist particles," *International Journal of Thermal Sciences,* vol. 42, pp. 691-701, 7. 2003.

[37] R. W. R. Zwart., H. Boerrigter and A. van der Drift., "The Impact of Biomass Pretreatment on the Feasibility of Overseas Biomass Conversion to Fischer− Tropsch Products," *Energy Fuels,* vol. 20, pp. 2192-2197, 2006.

[38] I. Hannula., "Hydrogen production via thermal gasification of biomass in near-to-medium term, Working paper 131, VTT Processes, Espoo, 2009." 2009.

[39] A. Faaij., "Gasification of biomass wastes and residues for electricity production," *Biomass Bioenergy,* vol. 12, pp. 387-407, 1997.

[40] J. Pierik and A. Curvers, "Logistics and pretreatment of biomass fuels for gasification and combustion," 1995.

[41] L. Fagernäs., J. Brammer., C. Wilén and C. Lauer., "Drying of biomass for second generation synfuel production," *Biomass Bioenergy,* 2010.

[42] M. E. Dry., "The Fischer–Tropsch process: 1950–2000," *Catalysis Today,* vol. 71, pp. 227-241, 1/15. 2002.

[43] H. Schulz, "Short history and present trends of Fischer-Tropsch synthesis," *Applied Catalysis A: General,* vol. 186, pp. 3-12, 1999.

[44] M. E. Dry., "High quality diesel via the Fischer-Tropsch processes, a review," *Journal of Chemical Technology & Biotechnology,* vol. 77, pp. 43-50, 2002.

[45] G. P. van der Laan and A. Beenackers., "Intrinsic kinetics of the gas–solid Fischer–Tropsch and water gas shift reactions over a precipitated iron catalyst," *Applied Catalysis A: General,* vol. 193, pp. 39-53, 2/28. 2000.

[46] Y. Wang, W. Ma, Y. Lu, J. Yang, Y. Xu, H. Xiang, Y. Li, Y. Zhao and B. Zhang, "Kinetics modelling of Fischer–Tropsch synthesis over an industrial Fe–Cu–K catalyst," *Fuel,* vol. 82, pp. 195-213, 1. 2003.

[47] G. P. Van Der Laan and A. Beenackers., "Kinetics and selectivity of the Fischer–Tropsch synthesis: a literature review," *Catalysis Reviews,* vol. 41, pp. 255-318, 1999.

[48] H. D. Burtron., "Overview of reactors for liquid phase Fischer–Tropsch synthesis," *Catalysis Today,* vol. 71, pp. 249-300, 1/15. 2002.

[49] C. Perego, "Development of a Fischer-Tropsch catalyst: From laboratory to commercial scale demonstration," *Rendiconti Lincei,* vol. 18, 2007.

[50] K. Jalama, N. J. Coville, D. Hildebrandt, D. Glasser and L. L. Jewell, "Fischer–Tropsch synthesis over Co/TiO2: Effect of ethanol addition," *Fuel,* vol. 86, pp. 73-80, 1. 2007.

[51] A. Tavasoli, A. Khodadadi, Y. Mortazavi, K. Sadaghiani and M. G. Ahangari, "Lowering methane and raising distillates yields in Fischer–Tropsch synthesis by using promoted and unpromoted cobalt catalysts in a dual bed reactor," *Fuel Process Technol,* vol. 87, pp. 641-647, 7. 2006.

[52] S. Sharifnia, Y. Mortazavi and A. Khodadadi, "Enhancement of distillate selectivity in Fischer–Tropsch synthesis on a Co/SiO2 catalyst by hydrogen distribution along a fixed-bed reactor," *Fuel Process Technol,* vol. 86, pp. 1253-1264, 8/25. 2005.

[53] M. E. Dry, "Fischer-Tropsch synthesis over iron catalysts," *Catalysis Letters,* vol. 7, pp. -12-13. 1990.

[54] M. E. Dry., "The Fischer-Tropsch Synthesis in Anderson, JR; M. Boudart, M.(eds.), Catalysis," *Science and Technology,* vol. 1, pp. 159-255, 1981.

[55] G. P. van der Laan., "Kinetics, selectivity and scale up of the Fischer-Tropsch synthesis," *NPT Procestechnologie, 2000 - Dissertations.Ub.Rug.Nl,* vol. 3, pp. 18–21, 2000.

[56] S. Srinivas, "Feasibility of Reactive Distillation for Fischer−Tropsch Synthesis. 2," *Ind Eng Chem Res,* vol. 48, pp. 4710-4718, 2009.

[57] V. U. S. Rao, G. J. Stiegel, G. J. Cinquegrane and R. D. Srivastava, "Iron-based catalysts for slurry-phase Fischer-Tropsch process: Technology review," *Fuel Process Technol,* vol. 30, pp. 83-107, 2. 1992.

[58] H. Schulz and M. Claeys, "Kinetic modelling of Fischer–Tropsch product distributions," *Applied Catalysis A: General,* vol. 186, pp. 91-107, 10/4. 1999.

[59] J. Gregor, "Fischer-Tropsch products as liquid fuels or chemicals," *Catalysis Letters,* vol. 7, pp. 317-331, 1990.

[60] A. Van der Drift and H. Boerrigter, "Synthesis gas from biomass for fuels and chemicals," in *SYNBIOS Conf. Stockholm, Sweden. may,* 2005, pp. 06-001.

[61] A. Fourcault, F. Marias and U. Michon, "Modelling of thermal removal of tars in a high temperature stage fed by a plasma torch," *Biomass Bioenergy,* vol. 34, pp. 1363-1374, 9. 2010.

[62] Milne. TA., Evans. RJ., Abatzaglou. N., "Biomass Gasifier"Tars": Their Nature, Formation, and Conversion," *Biomass Gasifier"Tars": Their Nature, Formation, and Conversion,* 1998.

[63] M. P. Houben, H. C. de Lange and A. A. van Steenhoven, "Tar reduction through partial combustion of fuel gas," *Fuel,* vol. 84, pp. 817-824, 5. 2005.

[64] J. Han and H. Kim, "The reduction and control technology of tar during biomass gasification/pyrolysis: An overview," *Renewable and Sustainable Energy Reviews,* vol. 12, pp. 397-416, 2008.

[65] J. Han and H. Kim, "The reduction and control technology of tar during biomass gasification/pyrolysis: An overview," *Renewable and Sustainable Energy Reviews,* vol. 12, pp. 397-416, 2. 2008.

[66] C. Li and K. Suzuki, "Tar property, analysis, reforming mechanism and model for biomass gasification—An overview," *Renewable and Sustainable Energy Reviews,* vol. 13, pp. 594-604, 4. 2009.

[67] L. Devi., K. J. Ptasinski., and F. J. J. G. Janssen., "A review of the primary measures for tar elimination in biomass gasification processes," *Biomass Bioenergy,* vol. 24, pp. 125-140, 2003.

[68] R. J. Evans., and T. A. Milne., "Molecular characterization of the pyrolysis of biomass," *Energy Fuels,* vol. 1, pp. 123-137, 1987.

[69] A. Dufour., P. Girods., E. Masson and Y. Rogaume., "Synthesis gas production by biomass pyrolysis: Effect of reactor temperature on product distribution," *Int J Hydrogen Energy,* vol. 34, pp. 1726-1734, 2. 2009.

[70] L. Devi., "Decomposition of Naphthalene as a Biomass Tar over Pretreated Olivine: Effect of Gas Composition, Kinetic Approach, and Reaction Scheme," *Ind Eng Chem Res,* vol. 44, pp. 9096-9104, 2005.

[71] P. Buchireddy., R. Bricka., J. Rodriguez and W. Holmes., "Biomass Gasification: Catalytic Removal of Tars over Zeolite and Nickel Supported Zeolite," *ENERGY and FUELS,* vol. 24, pp. 2707-2715, 2010.

[72] S. S. Pansare., Jr. J. G. Goodwin and S. Gangwal., "Toluene decomposition in the presence of hydrogen on tungsten-based catalysts," *Ind.Eng.Chem.Res.Industrial and Engineering Chemistry Research,* vol. 47, pp. 4077-4085, 2008.

[73] Z. Abu El-Rub., E. Bramer., G. Brem., "Review of Catalysts for Tar Elimination in Biomass Gasification Processes," *Industrial & Engineering Chemistry Research.,* vol. 43, pp. 6911, 2004.

[74] A. Olivares, M. P. Aznar, M. A. Caballero, J. Gil, E. Frances and J. Corella, "Biomass gasification: Produced gas upgrading by in-bed use of dolomite," *Industrial and Engineering Chemistry Research,* vol. 36, pp. pp. 5220-5226, 1997.

[75] D. Sutton, B. Kelleher and J. R. H. Ross, "Review of literature on catalysts for biomass gasification," *Fuel Process Technol,* vol. 73, pp. 155-173, 11/13. 2001.

[76] D. Dayton., "A Review of the Literature on Catalytic Biomass Tar Destruction," *Review of the Literature on Catalytic Biomass Tar Destruction: Milestone Completion Report,* 2002.

[77] H. Schmieder, J. Abeln, N. Boukis, E. Dinjus, A. Kruse, M. Kluth, G. Petrich, E. Sadri and M. Schacht, "Hydrothermal gasification of biomass and organic wastes," *The Journal of Supercritical Fluids,* vol. 17, pp. 145-153, 2000.

[78] P. Mondal., G. Dang., M. Garg., "Syngas production through gasification and cleanup for downstream applications — Recent developments," *Fuel Process Technol,* vol. 92, pp. 1395-1410, 8. 2011.

[79] E. Furimsky, "Gasification in Petroleum Refinery of 21st Century," *OIL AND GAS SCIENCE AND TECHNOLOGY,* vol. 54, pp. 597-618, 1999.

[80] J. Smid, S. Hsiau, C. Peng and H. Lee, "Hot gas cleanup: pilot testing of moving bed filters," *Filtration Sep.,* vol. 43, pp. 21-24, 5. 2006.

[81] V. Mohebbi, R. M. Behbahani and M. Moshfeghian, "Method calculates lean, semilean streams in split-flow sweetening," *Oil Gas J.,* vol. 105, pp. 70-79, 2007.

[82] B. Bhide., A. Voskericyan and S. Stern., "Hybrid processes for the removal of acid gases from natural gas," *J. Membr. Sci.,* vol. 140, pp. 27-49, 3/4. 1998.

[83] R. Idem, M. Wilson, P. Tontiwachwuthikul, A. Chakma, A. Veawab, A. Aroonwilas and D. Gelowitz, "Pilot Plant Studies of the CO2 Capture Performance of Aqueous MEA and Mixed MEA/MDEA Solvents at the University of Regina CO2 Capture Technology Development Plant and the Boundary Dam CO2 Capture Demonstration Plant," *Industrial & Engineering Chemistry Research.,* vol. 45, pp. 2414, 2006.

[84] K. Hyung., Y. Sung., K. Young and L. Bomsock., "Simulation of CO2 removal in a split-flow gas sweetening process," *Korean Journal of Chemical Engineering,* vol. 28, -02-26. 2011.

[85] M. Ruggiero and G. Manfrida, "An equilibrium model for biomass gasification processes," *Renewable Energy,* vol. 16, pp. 1106-1109, 4. 1999.

[86] C. Dupont., G. Boissonnet and S. Guillaume., "Study about the kinetic processes of biomass steam gasification," *Fuel,* vol. 86, pp. 32-40, 1. 2007.

[87] J. Corella and A. Sanz., "Modeling circulating fluidized bed biomass gasifiers. A pseudo-rigorous model for stationary state," *Fuel Process Technol,* vol. 86, pp. 1021-1053, 5/25. 2005.

[88] X. T. Li, J. R. Grace, C. J. Lim, A. P. Watkinson, H. P. Chen and J. R. Kim, "Biomass gasification in a circulating fluidized bed," *Biomass Bioenergy,* vol. 26, pp. 171-193, 2. 2004.

[89] Lü. Pengmei., X. Kong., C. Wu and Z. Yuan., "Modeling and simulation of biomass air-steam gasification in a fluidized bed," *Frontiers of Chemical Engineering in China,* vol. 2, -06-03. 2008.

[90] A.V. Bridgwater and G. D. Evans., *An Assessment of Thermochemical Conversion Systems for Processing Biomass and Refuse. Energy Technology Support Unit., University of Aston in Birmingham and DK Teknik (Denmark),[Harwell]: ETSU, 1993,* [Harwell]: ETSU, 1993,

[91] J. Michael Jr, "Cellulose Pyrolysis Kinetics: The Current State of Knowledge," *Ind Eng Chem Res,* vol. 34, pp. 703-717, 1995.

[92] R. P. Overend, T. A. Milne, L. K. Mudge and International Energy Agency., "Fundamentals of thermochemical biomass conversion," in 1985,

[93] A. Gomez-Barea and B. Leckner., "Modeling of biomass gasification in fluidized bed," *Prog.Energy Combust.Sci.,* vol. 36, pp. 444-509, 2010.

[94] D. Fiaschi and M. Michelini, "A two-phase one-dimensional biomass gasification kinetics model," *Biomass Bioenergy,* vol. 21, pp. 121-132, 8. 2001.

[95] JF. Davidson and D. Harrison., "Fluidized particles," *Mobile Particulate Systems,* pp. 173, 1995.

[96] I. G. T. C. D. Model, "IGT Coal Density Model," *Aspen Plus7,* 1976.

[97] J. Wang, M. Jiang, Y. Yao, Y. Zhang and J. Cao, "Steam gasification of coal char catalyzed by K2CO3 for enhanced production of hydrogen without formation of methane," *Fuel,* vol. 88, pp. 1572-1579, 9. 2009.

[98] R.K. Sinnott., J.M. Coulson and J.F. Richardson., *Coulson & Richardson's Chemical Engineering. Vol. 6, Chemical Engineering Design.* Oxford: Elsevier Butterworth-Heinemann, 2005,